MICROCOPY RESOLUTION TEST CHART
NATIONAL BUREAU OF STANDARDS-1963-A

ONR-TR

RE-654J

THEORETICAL AERODYNAMICS OF JETS IN GROUND EFFECT
PHASE V - ASYMPTOTIC THEORY OF TURBULENT WALL JETS

R.E. Melnik and A. Rubel
R&D Center
Grumman Aerospace Corporation
Bethpage, New York   11714

Final Report
for Period 15 June 1981 - 14 November 1982

April 1983

Prepared for

REPORT DOCUMENTATION PAGE		READ INSTRUCTIONS BEFORE COMPLETING FORM
1. REPORT NUMBER RE-654J	2. GOVT ACCESSION NO.	3. RECIPIENT'S CATALOG NUMBER
4. TITLE (and Subtitle) Theoretical Aerodynamics of Jets in Ground Effect Phase V - Asymptotic Theory of Turbulent Wall Jets		5. TYPE OF REPORT & PERIOD COVERED Final Report 6/15/81 - 11/14/82
		6. PERFORMING ORG. REPORT NUMBER ONR-TR
7. AUTHOR(s) R.E. Melnik and A. Rubel		8. CONTRACT OR GRANT NUMBER(s) N00014-81-C-0549
9. PERFORMING ORGANIZATION NAME AND ADDRESS Grumman Arospace Corporation Research and Development Center Bethpage, New York 11714		10. PROGRAM ELEMENT, PROJECT, TASK AREA & WORK UNIT NUMBERS 061-251
11. CONTROLLING OFFICE NAME AND ADDRESS Office of Naval Research 800 N. Quincy Street Arlington, VA 22217		12. REPORT DATE April 1983
		13. NUMBER OF PAGES
14. MONITORING AGENCY NAME & ADDRESS(if different from Controlling Office) SAME		15. SECURITY CLASS. (of this report) UNCLASSIFIED
		15a. DECLASSIFICATION DOWNGRADING SCHEDULE

16. DISTRIBUTION STATEMENT (of this Report)

Approved for public release; distribution unlimited

17. DISTRIBUTION STATEMENT (of the abstract entered in Block 20, if different from Report)

Approved for public release; distribution unlimited

18. SUPPLEMENTARY NOTES

19. KEY WORDS (Continue on reverse side if necessary and identify by block number)

Fluid mechanics
Wall jets
Asymptotic theory

20. ABSTRACT (Continue on reverse side if necessary and identify by block number)

This report presents a systematic analysis of two-dimensional and radial turbulent wall jets using the method of matched asymptotic expansions. The asymptotic solution is carried out in two stages. The first is based on a two parameter expansion of the full Reynolds averaged equations with a k-ϵ model of turbulence quantities. One of the small parameters, γ, is related to the nondimensional friction velocity, u, defined by the surface shear stress. It is basically a Reynolds number parameter $\gamma = 0 \, (\ln Re)^{-1}$, that primarily

controls the shear stress effects induced by the wall. The other small parameter, α, is related to the modeling constants arising in the chosen turbulence closure. In the present k-ϵ model analysis α is identified with the constant, c_μ, appearing in the eddy viscosity formula for the Reynolds shear stress and is a measure of the turbulence levels in the outer free jet part of the flow. The α expansion reduces the problem to a classical boundary layer formulation to lowest order. The expansion for $\gamma \to 0$ leads to a four layer description of the wall jet. The outer layer is closely related to a free jet flow while the innermost layer is a classical law of the wall region. Two additional intermediate layers are needed to effect the matching of the outer and inner layers and to complete the solution. Leading order solutions for each layer are presented and the composite flow field result is compared with an existing numerical solution for the wall jet.

Grumman Research Department Report RE-654J

THEORETICAL AERODYNAMICS OF JETS IN GROUND EFFECT
PHASE V - ASYMPTOTIC THEORY OF TURBULENT WALL JETS

Final Report on Contract N00014-81-C-0549
for Period 15 June 1981 - 14 November 1982

Prepared for

Office of Naval Research
Department of the Navy
800 N. Quincy Street
Arlington, Virginia 22217

April 1983

APPROVED FOR PUBLIC RELEASE: DISTRIBUTION UNLIMITED

Approved by: Richard A. Scheuing
Richard A. Scheuing
Director, R&D Center

ASYMPTOTIC THEORY OF TURBULENT WALL JETS

R.E. Melnik*
A. Rubel**
Research and Development Center
Grumman Aerospace Corporation
Bethpage, New York 11714

Abstract

This paper presents a systematic analysis of two-dimensional and radial turbulent wall jets using the method of matched asymptotic expansions. The asymptotic solution is carried out in two stages. The first is based on a two parameter expansion of the full Reynolds averaged equations with a k-ε model of turbulence quantities. One of the small parameters, γ, is related to the nondimensional friction velocity, u_τ, defined by the surface shear stress. It is basically a Reynolds number parameter, $\gamma = 0(\ln Re)^{-1}$, that primarily controls the shear stress effects induced by the wall. The other small parameter, α, is related to the modeling constants arising in the chosen turbulence closure. In the present k-ε model analysis α is identified with the constant, c_μ, appearing in the eddy viscosity formula for the Reynolds shear stress and is a measure of the turbulence levels in the outer free jet part of the flow. The α expansion reduces the problem to a classical boundary layer formulation to lowest order. The expansion for $\gamma \rightarrow 0$ leads to a four layer description of the wall jet. The outer layer is closely related to a free jet flow while the innermost layer is a classical law of the wall region. Two additional intermediate layers are needed to effect the matching of the outer and inner layers and to complete the solution. Leading order solutions for each layer are presented and the composite flow field result is compared with an existing numerical solution for the wall jet.

Nomenclature

a	Constant Defined by Eq. (45b)
$A(x)$	Function Appearing in Inner Limit of Outer Solution
A_s	Constant Appearing in Inner Limit of Outer Similarity Solution
b	Constant Given by $b = 1 - (3/2)a$
b*	Reference Length in Initial Jet
$B(x)$	Function Appearing in Inner Limit of Outer Solution
B_s	Function Appearing in Inner Limit of Outer Similarity Solution
c_f	Skin Friction Coefficient Based on Initial Jet Conditions
c_F	Skin Friction Coefficient Based on $u_w(x)$
$c_w(x)$	Function Defined by Eq. 40 $(c_w = u_w\, du_w/dx)$
$\bar{c}(x)$	Function Appearing in Transition Layer Solution, Defined by Eq. (80a)
$c_{\varepsilon 1}, c_{\varepsilon 2}$	Turbulence Model Constants ($c_{\varepsilon 1} = 1.44$, $c_{\varepsilon 2} = 1.92$)
c_μ	Function of P/ε and f Defining Turbulent Viscosity

$c_{\mu o}$	Turbulent Model Constant ($c_{\mu o} = 0.09$)
C_J	Momentum Flux Constant Defined by Eq. (32)
C^+	Constant in Law of the Wall, Eq. (103)
d	Constant Defined by Eq. (100)
e	Constant Defined by Eq. (101)
$E(\varsigma)$	Similarity Function for Dissipation, Transition Layer Eq. (84)
E_s	Constant in Similarity Solution for Dissipation, Transition Layer
f	Wall Damping Function Defined by Eq. (3)
$F(\eta)$	Streamfunction in Similarity Solution, Outer Layer, Eq. (25) - (26)
g	Normalized Reynolds Shear Stress Defined by Eq. (10c)
$G(\eta)$	Similarity Function for Turbulent Energy - Outer Layer, Eq. (27)
$\bar{G}$	Function Defining Turbulent Viscosity in Transition Layer, Eq. (86)
G_μ	Function Defining Turbulent Viscosity Eq. (2)
$G_{\mu w}, G_{\mu o}$	Limit Values of Turbulent Viscosity Function Defined by Eqs. (43) and (47)
$H(\eta)$	Similarity Function for Dissipation - Outer Layer, Eq. (29)
j	Index Equal to 0 for Plane Jet, Equal to 1 for Radial Jet
J	Momentum Flux Defined by Eq. (24)
k	Normalized Turbulent Energy, Eq. (10d)
$K(\eta), K(\varsigma)$	Similarity Functions for Turbulent Energy - Outer Layer Eq. (28) and Transition Layer Eq. (83)
P	Turbulent Production, $\nu_t(\partial U/\partial y)^2$
r	Nondimensional Coordinate along the Wall ($r = r*/b*$)
Re_j	Jet Reynolds Number ($u_j*b*/\nu*$)
u	Velocity in the x, r Direction - Outer Solution Eq. (17)
u_w	Velocity at the Wall ($y = 0$)- Outer Layer Solution
u_τ	Friction Velocity $\sqrt{\tau_w} = \sqrt{c_f/2}$
U	Velocity Component in x, r Direction, Eq. (10a)
U_m	Maximum Velocity in Streamwise Velocity Profile
v	Velocity in y Direction - Outer Solution, Eq. (18)
V	Nondimensional Velocity Component in y Direction, Eq. (10b)
x	Stretched Coordinate in r Direction, Eq. (11)
y	Nondimension Coordinate Normal to Plate, Eq. (11)
y_m	Coordinate of Velocity Maximum
α	Small Parameter Equal to $c_{\mu o}$
$\Gamma(K)$	Function Appearing in Transition Layer Similarity Solution Eq. (80)
β_w	Value of β at the Wall, y = 0, Eq. (107)
γ	Small Parameter, $\gamma = u_\tau r/\varepsilon^{(1+j)/4}$
$\delta_m, \delta_{1/2}$	Y Coordinate Value of Wall Jet Edge, Maximum Velocity, and Half Velocity Point
$\varepsilon_1(x), \varepsilon_2(x)$	Functions Appearing Diffusion Layer Solutions, Eqs. (63) - (64)
	Normalized Turbulent Dissipation Defined by Eq. (10e)

---

*Director for Fluid Mechanics
**Head, Theoretical Aerodynamics Laboratory

1

η	Similarity Coordinate - Outer Layer, Eq. (30)
$\gamma(x)$	Function Appearing in Solution for Skin Friction Eq. (115a)
γ_s	Constant Appearing in Solution for Skin Friction Eq. (115b)
κ	von Karmen Constant ($\kappa = 0.43$)
κ_1	Scaled Von Karmen Constant ($\kappa_1 = \kappa a^{-1/4} = 0.80$)
λ	Constant, $\lambda = (\sigma_\varepsilon/\sigma_k)\, c_{\varepsilon 2}$, Eq. (45b)
Λ	Local Skin Friction Parameter, $\Lambda = a^{1/4}\sqrt{\tau_w}/\kappa u_w$
ν_t	Turbulent Viscosity, Eq. (1)
ν	Laminar Viscosity
ρ	Density
$\sigma_k, \sigma_\varepsilon$	Turbulent Model Constants ($\sigma_k = 1$, $\sigma_\varepsilon = 1.3$)
τ_w	Skin Friction
$\tau_{w,r}$	Reference Value of Skin Friction
$\bar{\tau}_w$	Normalized Skin Friction $\bar{\tau}_w = \tau_w/\tau_{w,r}$

Superscripts

$\sim$	Denotes Diffusion Layer Quantities
$-$	Denotes Transition Layer Quantities
$'$	Prime - Denotes Derivative with Respect to Similarity Variables, η, ζ
$*$	Denotes Dimensional Variable
$+$	Wall Layer Variable
(0)	Perturbation Index

Subscripts

D	Diffusion Layer Solution
e	Wall Set Edge Value
m	Denotes Value at the Maximum of the Streamwise Velocity
w	Value at Wall (y, $\tilde{y}$, $\bar{y} = 0$)
o	Perturbation Index
cp	"Common Part"

I. Introduction

In this paper we examine the theoretical structure of radial and planar wall jets spreading out on a flat surface in stagnant surroundings. Although geometrically simple, these flows raise many theoretical questions relating to turbulence modeling and to wall jet similarity and asymptotic structure. Wall jets are of interest in turbulence modeling because they combine in a single flow field important aspects of both free and wall bounded turbulence. They are also simple examples of a flow with a velocity maximum that is not coincident with a vanishing turbulent shear stress; a feature that cannot be described by turbulence models employing an eddy viscosity hypothesis.

As discussed, for example, by Townsend[1] turbulent wall jets developing in stagnant surroundings belong to a general class of flows referred to as self-preserving. Such a flow is similar (or self-preserving) if the form of the solution, when non-dimensionalized with respect to certain velocity and length scales, is independent of r, the coordinate parallel to the shear layer. These velocity and length scales are usually simple power law functions of the streamwise coordinate. The similarity transformation reduces the original partial differential equations to ordinary differential equations. If the similarity is exact, the solutions of the ordinary differential equations are also exact solutions of the original governing equations. The conditions that need to be satisfied for similar solutions to exist in turbulent flow are discussed by Townsend[2], Rotta[3], Rodi[4] and many others. Examples of similarity solutions in free turbulent flows are well known (e.g. jets, mixing layers) and are given in standard fluid mechanics texts (e.g. Ref. 5). Wall bounded turbulent flows generally do not satisfy the conditions for exact similarity except in very special circumstances that are much more restrictive than in laminar flow.

Wall bounded flows, however, do exhibit a more general form of similarity referred to as asymptotic similarity. In this case, if the external conditions permit it, the boundary layer approaches a similar state far downstream. The similar solution is then the leading term in an asymptotic, coordinate type expansion, valid for $r \to \infty$. In this case, the leading order similarity solution is generally not an exact solution of the original governing equations but is only an approximation that becomes more exact as distance increases. Nonsimilar effects arise from higher order terms of the underlying asymptotic expansions. As is well known, turbulent wall layers develop in a multi-layer structure consisting of two or more layers. The solution in each layer can be developed in a far field similarity form, but the form of the similarity solution and the velocity and length scales differ in each of the layers. Thus, the overall solution never achieves a completely self-preserving asymptotic state because the solution in each region develops at a different rate. Nevertheless the solution in each region correctly matches its neighbors, in the sense of the method of matched asymptotic expansions, and the overall solution is a rational asymptotic solution valid far downstream.

Glauert[6] developed an approximate analytic solution for both planar and radial wall jets in still air. He was able to construct a solution in near-similarity form by assuming the flow to be divided into two regions: an outer free jet type flow, and an inner conventional turbulent boundary layer. The two solutions were matched at the position of the velocity maximum where the turbulent Reynolds stresses were also assumed to vanish. The solution in the outer layer was obtained with a constant eddy viscosity model appropriate to free jet flows while the solution in the inner layer was assumed to be the same as in turbulent pipe flow. Townsend[1] also developed a near-similar two layer solution for the wall jet but he employed a standard logarithmic wall layer for the inner solution instead of the power law profile used by Glauert. Comparison of Glauert's theory with experiment shows that it can accurately predict the velocity profiles and most other features of the flow. The theory indicates that the inner and outer layers grow at slightly different rates and that the exponents in the velocity and length scales slightly differ from the similarity values of free jets. These effects are due to the approximate nature of the similarity of wall jets.

Two controversial aspects of the theoretical solution are the values of the exponents in the velocity and length scales and the question of the existence of a logarithmic behavior in the velocity profile near the wall. For a radial free jet, the similarity solutions indicate that the length scale, $\delta_{1/2}$, increases linearly with radial distance, r, while the velocity scale, u_m decays as r^{-1}. The experimental results of Bakke[7] and Poreh, Tsuei and Cermak[8] for radial wall jets are consistent with Glauert's prediction for the velocity scale, both showing a 10-15% decrease

2

in the exponent from the similarity value. However, the same data also indicates a 5 to 10% decrease in the exponent of the length scale for which the Glauert theory predicts a 2% increase above the similarity value. For the planar free jet the similarity exponent for the velocity scale is -1/2 while that for the length scale is 1 which is the same as the value in a radial jet. The data for the velocity scale in planar wall jets was summarized by Hammond[9]. The experimental results indicated a decrease of exponent in the velocity scale by about 5-10% from the similarity value which, as in the radial case, is consistent with Glauert's theory. The results for the length scale in the planar case are somewhat equivocal. The experimental results of Schwarz and Cosart[10] and Meyers, Schauer and Eustis[11] indicate that the exponent for the length scale is equal to the similar-ity value, 1, while the Bradshaw and Gee[12] data indicate a value 10% lower.

There is considerable uncertainty as to whether a conventional logarithmic law of the wall region de-velops in the velocity profile of a wall jet. The same theoretical arguments that support a log law in boundary layers and pipe flows suggests that it should also arise in wall jets. However, the experi-mental results of Bradshaw and Gee[12], Poreh, Tsuei and Cermak[8], Schwarz and Cosart[10], and others, as well as the analysis of Hammond[9] all indicate that wall jets do not exhibit a well defined log law region. These results indicate that, if a log law profile exists at all, it must extend only over a very narrow region, and with constants that differ significantly from the standard values appropriate to boundary layers and pipe flows. Nevertheless, a conventional log law behavior was assumed in setting the boundary con-ditions in recent calculations by Ljuboja and Rodi[13] using the k-ε model for a wall jet on flat surface and by Gibson and Younis[14] in calculations with a Rey-nolds stress model on curved surfaces.

Wall jets are known to spread less rapidly than free jets. Ljuboja and Rodi[13] note that the reduced spread rate of wall jets could not be accounted for with the standard k-ε model employing the same con-stants that successfully predict free jet flows. The standard k-ε model overpredicts the wall jet spread rate by 30 percent. They suggest that this failure is due mainly to the inadequacies of the turbulence model with regard to the "damping" effect of the wall on the normal velocity fluctuations rather than due to the direct action of the wall shear stress. Their results, obtained with a modified k-ε model that ac-counted for the wall damping effect, showed much improved predictions of the spread rate.

In order to address the foregoing issues we thought it desirable to develop a more rigorous ana-lytical solution of the wall jet problem. In the present paper we will not be concerned with turbulence modeling per se. The turbulence modeling aspects of the wall jet problem have recently received much attention and the available data and turbulence models have been evaluated at the 1980-81 AFOSR Stanford conference on complex turbulent flows[15]. Instead, in the present paper we are concerned with the overall theoretical structure of wall jet flows and with the development of a general theoretical ap-proach to this class of flows. In order to keep the analysis as simple as possible and to produce definite results that can be compared with available numeri-cal solutions we've based the present study on the standard k-ε model including the wall damping modi-fications proposed by Ljuboja and Rodi[13]. The pres-ent theoretical study indicates that a key feature of

the wall jet flow is that the Reynolds stresses in the outer layer are an order of magnitude larger than the levels near the wall. The analysis to follow will show that this feature dominates the theoretical develop-ment and leads to a characteristic multi-layer struc-ture that is typical for flows with relatively large Reynolds stress levels in the outer region. We be-lieve that the theoretical approach developed here is general and may prove useful for analyzing other flows with the k-ε or other turbulence models.

Our approach to the wall jet problem is based on a rational asymptotic analysis of the k-ε model equations using the method of matched asymptotic expansions. It is an outgrowth of the asymptotic methods developed for boundary layers and for vari-ous turbulent viscid inviscid interaction problems (see Refs 16, 17 for a review of this latter work). In all of these works the solution was developed as an asymptotic expansion in terms of the Reynolds number, or equivalently in terms of a reference value of the friction velocity. In these problems the asymptotic approach leads to a multi-layer struc-ture with the velocity in the outer part of the bound-ary layer developing a small defect form. The pres-ent work represents a significant departure from these studies in that the velocity profile in the outer region of a wall jet is not in a small defect form. Be-cause of this, the wall jet develops a multi-layer structure that is considerably more complex than that which arises in a boundary layer.

In the present paper we are primarily inter-ested in the solution in the far field, similarity region. The asymptotic solution is carried out in two stages. The first is based on a two parameter expansion of the full Reynolds averaged equations with a k-ε model of turbulence quantities. One of the small parameters, γ, is related to the nondimen-sional friction velocity, u_τ, defined by the surface shear stress. It is basically a Reynolds number parameter, $\gamma = O(\ln Re)^{-1}$, that primarily controls the shear stress effects induced by the wall. The aforementioned asymptotic theories for boundary layers and flow in pipes are basically expansions in this parameter. The other small parameter appear-ing in our analysis, ε, is a measure of the turbu-lence levels in the outer free jet part of the flow. For Reynolds numbers approaching infinity, the wall jet flow approaches a limiting inviscid (Reynolds number independent) turbulent state that is closely related to classical free jet flows. Since for Re → ∞ there are no other nondimensional parameters appear-ing in the underlying deterministic governing equa-tions, ε must be a basically statistical parameter in-troduced by the coarse graining or averaging of the turbulent flow. Our analysis indicates that the ε→0 limit leads to a standard boundary layer de-scription with ε filling the role of the nondimen-sional viscosity coefficient (i.e. Re⁻¹). The value of ε is related to the modeling constants arising in the chosen turbulence closure. In the present analysis, in which we employ the k-ε model, ε is identified with the constant, c_μ, appearing in the eddy viscosity formula for the Reynolds shear stress. The constant c_μ is usually given by c_μ = 0.09 which is not impressively small for an asymptotic analysis. Nevertheless, the use of a small c_μ as ymptotic approach is plausible since its main effect is to reduce the Reynolds averaged equations to boundary layer form. This is known to be a generally useful approximation for both free and wall bounded turbulent flows, although not nearly as good as for laminar flows.

3

Thus, in the first stage of the analysis we expand the k-ε version of the full Reynolds averaged equations for γ, α→0. The α expansion reduces the problem to a classical boundary layer formulation to lowest order. The expansion for γ→0 leads to a four layer description of the wall jet. The outer layer is closely related to a free jet flow while the innermost layer is a classical law of the wall region. Two additional intermediate layers are needed to effect the matching of the outer and inner layers and to complete the solution. The analysis leads to a set of either partial or differential equations governing the solution in each region. The resulting description applies to the complete development of the wall jet flow, both in the near and far field, except for the immediate vicinity of an impingement region, where the boundary layer approximation of constant pressure across the shear layer is not valid.

In the second stage of our analysis we expand the solution in each layer in terms of distance along the wall to obtain a far field solution in each region. The leading order far field solution in each layer is expressible in a similarity form which turns out to be an exact solution of the equations governing the solution in each layer.

One of the interesting consequences of our approach concerns the character of the far field solution in the outermost layer of the wall jet. Because turbulent shear stress levels in the outer region are large, 0 (α), compared to the 0 (u²) levels in the inner wall layers, the turbulent shear stress in the outer solution must satisfy a zero boundary condition at the wall. This, together with the fact that the normal component of velocity is also zero at the wall leads to an outer solution that is similar in many respects to a symmetrical free jet flow. Because the turbulent shear stress vanishes at the wall, the momentum flux is conserved in the outer layer of the wall jet. to lowest order. Consequently the outer solution has the same similarity form in the far field as a free jet and the exponents in the velocity and length scales are equal to the free jet similarity values. However, the outer layer solution differs from the free jet solution because the presence of the wall directly influences the outer solution through the wall boundary conditions on the turbulent energy, k, and dissipation, ε, leading to a zero turbulent viscosity at the wall. Because of these boundary conditions the wall jet profiles in the outer region differ considerably from those of a free jet solution, particularly near the symmetry plane. It is also of interest to note that the difference in the wall boundary conditions for k and ε considerably decrease the spreading rate of the wall jet compared to a free jet, as is observed in practice.

The solution in the innermost region is represented by the conventional law of the wall formula. The overlap with its neighboring layer yields a conventional log law behavior with standard values assumed for the associated constants. However, because of the rapid variation of the solution in the other layers near the wall the extent of the log law overlap is much reduced compared to that in standard turbulent boundary layers and this tends to support the experimental findings reported previously[8,10,12].

In the present work we've developed a complete formulation, including the matching, for the leading order solution in each of the four layers. We've reduced the governing equations in each layer to far field similarity form and have obtained solutions for all the resulting ordinary differential equations.

We compare certain features of our far field solution with numerical solutions of the partial differential equations for the wall jet problem recently published by Ljuboja and Rodi[13] using the same form of k-ε turbulence model. We also compare our solutions for the velocity and length scales with the experimental correlations for planar wall jets presented by Narasimha, Yenga Narayan and Parthasarathy[18]. It is of interest to note that the present theory leads to the same similarity variables proposed by those authors on the basis of a dimensional analysis of the data and on the recognization that the initial momentum flux is the only relevant initial condition affecting the far field solution.

The solutions developed to date deal only with the leading order far field similarity solution and hence predict velocity and length scales that vary in accordance with the similarity values for the exponents. In order to address the nonsimilar effects associated with the shifts in velocity and length scale exponents observed in the data we would need to determine the next terms in the far field similarity expansions. Current efforts are directed at the computation of these terms.

II. Governing Equations. Asymptotic Formulation and Structure

We assume the wall jet is formed, either by impinging a jet onto a flat surface or by blowing through a narrow slot located near the origin as shown in Fig. 1. The initial conditions of the jet are characterized by velocity and length scales u_j^* and b^*, where these are dimensional quantities. All other quantities referred to in the paper are made dimensionless using these scales and the value of density in the initial jet. The quantities u_m and δ_m are the value and position of the maximum velocity while $\delta_{1/2}$ denotes the position of the half velocity point. Our analysis is based on the Reynolds averaged equations using the version of the k - ε model employed by Ljuboja and Rodi[13] in their numerical study of the planar wall jet. Their version includes modifications to account for: the wall "damping" effect, and the effect of the ratio of production to dissipation, P/ε, on the turbulent viscosity coefficient, ν_t. We closely follow the Ljuboja and Rodi[13] formulation and notation except for a minor change in the continuity equation to allow for the radial wall jet. In their formulation the turbulent viscosity coefficient is written in the form

$$\nu_t^* = c_\mu k^{*2}/\varepsilon^* \nu^* \qquad (1)$$

where the function c_μ is given by

$$c_\mu = c_{\mu_0} G_\mu(P/\epsilon, f) \qquad (2)$$

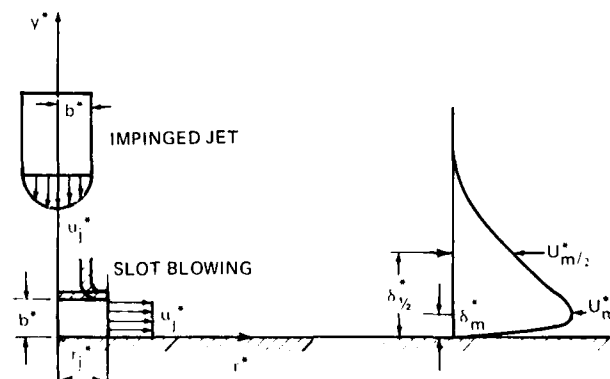

Fig. 1 Wall Jet in Still Air

And $c_{\mu 0}$ is one of the turbulence model constants (taken to be equal to $c_{\mu 0} = 0.09$), $G_\mu \equiv G_1 G_2$ is defined in Ljuboja and Rodi and f is their wall "damping" function,

$$f = MIN\left\{1, \frac{k^{*3/2} c_\mu^{3/4}}{y^* \epsilon^*}\right\} \qquad (3)$$

in here κ is the von Karmen constant.

The asymptotic analysis is carried out in terms of two basic small parameters, α and γ. The "boundary layer" parameter α is defined to equal $c_{\mu 0}$,

$$\alpha \equiv c_{\mu_0} = 0.09 \qquad (4)$$

while the "friction parameter" γ is defined in terms of a reference value of the nondimensional friction velocity, u_τ, by

$$\gamma \equiv u_{\tau, r}/\alpha^{(1+j)/4} \qquad (5)$$

where the friction velocity is defined by

$$u_\tau = \sqrt{\tau_w} = \sqrt{c_f/2} \qquad (6)$$

From turbulent wall layer flows we know that the friction velocity depends logarithmically on the Reynolds number Re_j,

$$u_\tau = O(\ln Re_j)^{-1} \qquad (7)$$

where

$$Re_j = u_j^* b^*/\nu^* \qquad (8)$$

In our approach, we seek solutions of the full Reynolds averaged equations in the double limit,

$$\alpha \to 0, \quad \gamma \to 0 \qquad (9)$$

Typical numerical values for these parameters for practical wall jet flows are $\alpha, \gamma \simeq 0.1$. Since these values are not impressively small we expect the higher order terms to be important in most situations. Nevertheless, we assume they are small enough for an asymptotic approach to be useful.

The parameter, α, enters the formulation in virtually the same manner as the laminar viscosity coefficient, and therefore expansion of the solution in powers of α leads to the boundary layer equations just as in laminar flow. The α expansion takes the form

$$U^*/u_j^* \alpha^{1/4} \equiv U = U^{(0)}(x, y; \gamma) + O(\alpha^{1/2}) + O(\alpha) \qquad (10a)$$

$$V^*/u_j^* \alpha^{(2+j)/4} \equiv V = V^{(0)}(x, y; \gamma) + O(\alpha^{1/2}) + O(\alpha) \qquad (10b)$$

$$-\langle u^* v^*\rangle/u_j^{*2}\alpha^{(1+j)/2} \equiv g = g^{(0)}(x, y; \gamma) + O(\alpha^{1/2}) + O(\alpha) \qquad (10c)$$

$$k^*/\rho^* u_j^{*2} \alpha^{1/2} \equiv k = k^{(0)}(x, y; \gamma) + O(\alpha^{1/2}) + O(\alpha) \qquad (10d)$$

$$\epsilon^* b^*/\rho^* u_j^{*3} \alpha^{(2+3j)/4} \equiv \epsilon = \epsilon^{(0)}(x, y; \gamma) + O(\alpha^{1/2}) + O(\alpha) \qquad (10e)$$

$$f = f^{(0)} + \cdots = \frac{k^{(0)3/2} G_\mu^{(0)3/4}}{\kappa_1 y \epsilon^{(0)}} + \cdots \qquad (10f)$$

$$G_\mu = G_\mu^{(0)}\{P^{(0)}/\epsilon^{(0)}, f^{(0)}\} + \cdots \qquad (10g)$$

where κ_1 is a "reduced" von Karmen constant defined by, $\kappa_1 = \kappa \alpha^{-1/4}$, and, x, y are stretched coordinates defined by

$$r^*/b^* = r = x \alpha^{-1/2}, \quad y^*/b^* = y \qquad (11)$$

where * denote dimensional quantities. We call attention to the appearance of the scaling parameter, α, in the definitions of the dependent variables. The j dependence follows from a consideration of the balance of the overall momentum flux. We also note that the boundary layer scaling appears in the r coordinate direction with the thickness of the wall jet equal to the order of magnitude of the slot width or other characteristic dimension of the impinging jet. This scaling implies that the solution holds in a region that is far downstream compared to the characteristic dimension of the initiating jet. The substitution of Eqs. (10) into the full Reynolds averaged equations, using the above stretchings, and taking the limit $\alpha \to 0$ leads to the standard boundary layer form of the equations of mass, momentum, turbulent energy and dissipation, written in the form, (with the perturbation superscripts deleted for simplicity)

$$\frac{\partial U}{\partial x} + \frac{\partial V}{\partial y} + \frac{jU}{x} = 0 \qquad (12)$$

$$U\frac{\partial U}{\partial x} + V\frac{\partial U}{\partial y} = \frac{\partial g}{\partial y} + Re_j^{-1}\frac{\partial^2 U}{\partial y^2} \qquad (13)$$

$$U\frac{\partial k}{\partial x} + V\frac{\partial k}{\partial y} = \frac{\partial}{\partial y}\left(\frac{\nu_t}{\sigma_k}\frac{\partial k}{\partial y}\right) + \nu_t\left(\frac{\partial U}{\partial y}\right)^2 - \epsilon \qquad (14)$$

$$U\frac{\partial \epsilon}{\partial x} + V\frac{\partial \epsilon}{\partial y} = \frac{\partial}{\partial y}\left(\frac{\nu_t}{\sigma_\epsilon}\frac{\partial \epsilon}{\partial y}\right) + c_{\epsilon 1}\frac{\epsilon \nu_t}{k}\left(\frac{\partial U}{\partial y}\right)^2 - c_{\epsilon 2}\frac{\epsilon^2}{k} \qquad (15)$$

The Reynolds stress, g, is computed from the mean velocity via an eddy viscosity formula,

$$g = \nu_t \frac{\partial U}{\partial y}, \quad \nu_t = G_\mu k^2/\epsilon \qquad (16)$$

with the eddy viscosity given by Eq. (1). We use standard values of the model constants given by: $c_{\mu 0} = 0.09$, $\sigma_k = 1$, $\sigma_\epsilon = 1.3$ $c_{\epsilon 1} = 1.44$ and $c_{\epsilon 2} = 1.92$. The α expansion provides the formal basis for using boundary layer theory for free turbulent flows as well as for the wall jet flow considered in this paper. The second term in the α expansion, Eq. (10), arises from small pressure gradients generated in the outer entrainment flow field above the wall jet. The disturbances in this region are induced by the entrainment of external fluid into the wall jet. The $O(\alpha)$ terms are due to higher order terms (i.e. normal pressure gradient, streamwise diffusion etc.) in the Reynolds averaged equations that are not included in the boundary layer equations.

The γ dependence in the solution indicated in Eq. (10) arises from the laminar shear stress term in Eq. (13), which is important only in the wall layer near the surface. The expansion for $\gamma \to 0$ leads to a solution with the complex four layer structure sketched in Fig. 2, consisting of: an outer free jet type flow, a conventional equilibrium wall layer, and two additional layers that are needed to effect a matching between the outer and inner layers. The solution in the outer layer satisfies the exact boundary layer equations. The Reynolds number term appearing in the momentum equation is negligible to

5

all orders in the outer expansion so that the outer layer is a fully turbulent flow that is not directly influenced by the laminar viscosity coefficient. Of course, there are Reynolds number effects in the outer solution, but they enter only through the inner matching conditions. The length scale for the outer region, $\Delta y = 0(1)$, indicated in Fig. 2, follows from boundary layer type scaling considerations. Since the spread rate of the wall jet is $0(\alpha^{1/2})$, the thickness of the outer layer, up to a distance $\Delta r = 0(\alpha^{-1/2})$ must be the same order as the characteristic dimension of the initial jet. Since the turbulent shear stress and energy are an order of magnitude larger than the $0(\gamma^2 \alpha^{(1+j)/2} = 0(u_\tau^2)$ levels at the wall, the outer solution for g and k must vanish at the wall. From the momentum equation it also follows that the outer solution for g must have a linear behavior near the wall. Detailed analysis, summarized in the following section, indicates that the outer solutions for the turbulent energy and dissipation have a non-analytic, algebraic behavior near the wall.

The solution in the innermost layer is described by a conventional equilibrium wall layer that is completely determined by the small, $0(\gamma^2 \alpha^{(1+j)})/2$ value of the wall shear stress. The solution in the wall layer has a standard logarithmic law of the wall behavior at its upper limit, $y_+ \equiv y u_\tau/\nu \to \infty$. Because of the algebraic behavior of the outer solution for $y \to 0$, the outer and wall layer solutions do not match and additional intermediate layers are required. Two additional layers are needed: a diffusion layer, and a transition layer. The thickness of the diffusion layer is determined by the condition that the linearly varying part of the solution for the shear stress is of the same order of magnitude as the value of the wall shear stress. This leads to a thickness $\Delta y = 0(\gamma^2)$ as indicated in the figure. This is the region

in which the velocity has a maximum and the turbulent shear stress has a zero. We call it a diffusion layer because of the dominant influence of turbulent diffusion in this layer. Detailed analysis indicates that the dissipation is balanced entirely by turbulent diffusion in this region. The dominant terms in the turbulent energy and diffusion equations in each layer are indicated in Fig. 2 by the symbols: A (advection), P (production), D_F (diffusion), and D_ε (dissipation).

The solution of the diffusion layer equations also exhibits an algebraic behavior at the wall which does not match the logarithmic behavior of the wall layer solution. This requires the introduction of the transition layer indicated in Fig. 2. The length scale, $\Delta y = \gamma^{2/a}$, for this layer is determined by the requirement that it matches to both the diffusion and wall layer solutions. The constant "a" is a function of the turbulence modeling constants, which for the standard values listed previously is given by, $a \approx 0.27$.

III. Outer Region

The solution in the outer region is determined by expanding the boundary layer equations, Eqs 12-16, in terms of the friction parameter, γ. Since the viscous term appearing in the momentum equation is exponentially small in γ it can be neglected to all orders. Thus, the leading order term in the outer solution satisfies the exact boundary layer equations with the laminar shear stress term set to zero. We assume that the solution in the outer region can be expanded in the form,

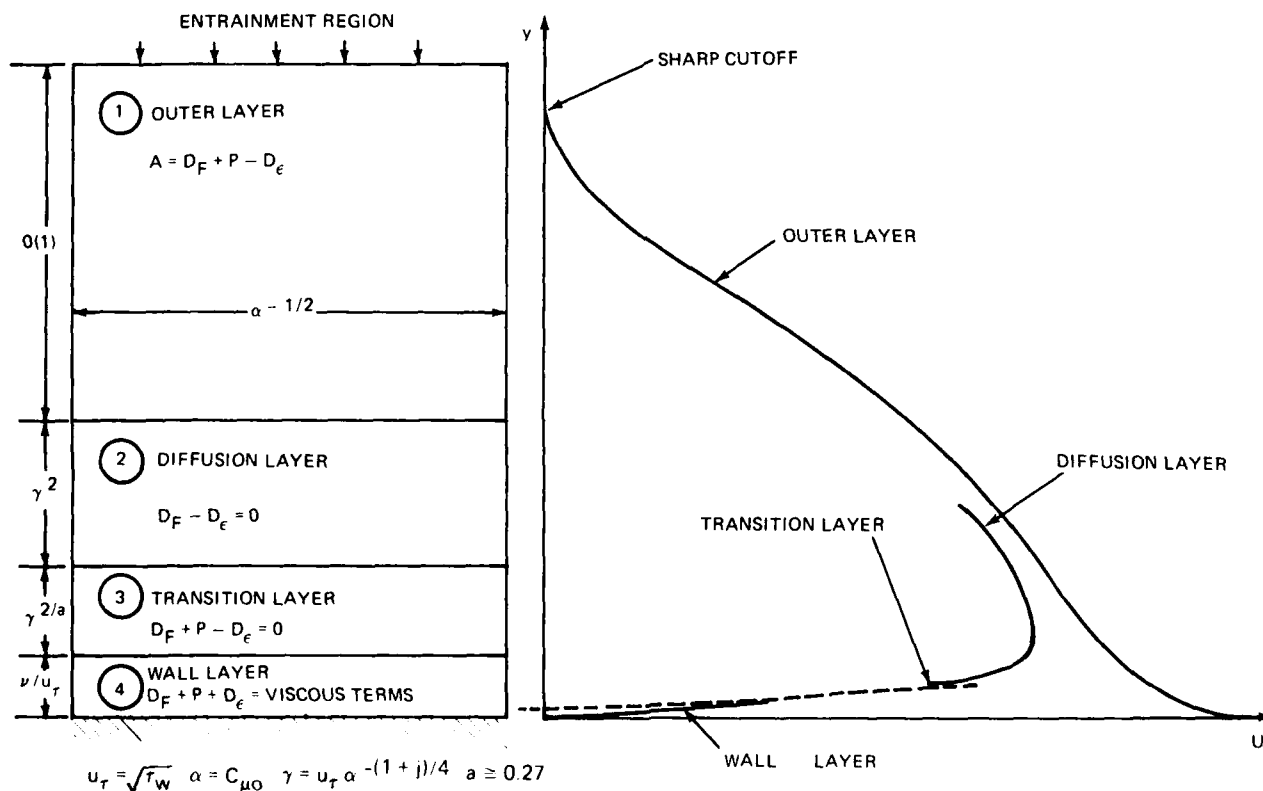$$U(x, y; \gamma) = u_0(x, y; 0) + \cdots \qquad (17)$$

Fig. 2 Wall Jet Flow Field Structure

$$V(x, y; \gamma) = v_0(x, y; 0) + \cdots \qquad (18)$$

$$g(x, y; \gamma) = g_0(x, y; 0) + \cdots \qquad (19)$$

$$k(x, y; \gamma) = k_0(x, y; 0) + \cdots \qquad (20)$$

$$\epsilon(x, y; \gamma) = \epsilon_0(x, y; 0) + \cdots \qquad (21)$$

and, for simplicity, we drop the perturbation subscripts in the subsequent developments.

For a stagnant outer stream the $k - \epsilon$ model leads to a shear flow with a definite outer edge, $y = y_e$, (e.g. see Ref. 19) where the solution satisfies homogeneous boundary conditions

$$u = g = k = \epsilon = 0 \quad \text{AT} \quad y = y_e \qquad (22)$$

The boundary conditions on the inner edge of the outer solution are determined by matching to the inner layers. Since g and k are $0 \ (\gamma^2)$ at the wall (and are also small in the other inner layers) the outer solution for these quantities must satisfy zero boundary conditions at the wall. The boundary condition on the dissipaton, ϵ, is more difficult to fix since it cannot be determined from simple scaling arguments if it should be equal to zero, infinite or a finite value at the wall.

A detailed analysis of the limiting behavior of the outer solution for $y \rightarrow 0$ indicates that matching is possible only if the dissipaton in the outer solution is unbounded at the wall. The final inner boundary condition is fixed by the requirement that the normal component of velocity be zero at the wall. Thus the inner boundary conditions are

$$v = g = k = 0 \qquad \text{AT} \quad y = 0 \qquad (23a)$$

$$\epsilon \rightarrow \infty \qquad \text{AT} \quad y = 0 \qquad (23b)$$

The boundary conditions given in Eqs. (22) and (23) are sufficient to completely determine the solution. As in the free jet problem, an additional wall boundary condition on u is not required because the wall value of u is determined from an overall momentum balance. Since the wall shear and normal component of velocity are zero at the wall the momentum flux integral, J, is constant to lowest order

$$J^* / \rho^* u_j^{*2} b^{*j+1} = J = (2-x)^j \int_0^{y_e} u^2(x, y; 0)\, dy + O(\gamma^2) \qquad (24)$$

where the $0 \ (\gamma^2)$ term arises from the nonzero value of the wall shear stress. The value of the momentum flux is set by the initial conditions in the impingement region.

The above boundary conditions completely define the outer solution, independent of the solution in the inner regions. However, the partial differential equations governing the outer solution must be integrated numerically as an initial value problem for each prescribed value of the momentum flux, J, and set of initial profiles. The solution in the region, $r^* = 0 \ (b^{*} \epsilon^{1/2})$ under consideration depends on the details of the initial profile shapes, which can only be determined from consideration of the detailed solution in the impingement region.

Far Field Similarity

Because the leading order solution for the shear stress vanishes at the wall, the momentum flux is constant to lowest order in γ, and consequently, the outer solution behaves very much like a turbulent free jet. In particular, the outer solution for the wall jet admits a similarity structure that is of the same form as that for a free jet. Thus the lowest order outer solution for the streamwise and normal components of velocity, turbulent energy and dissipation can be represented in the form,

$$u = u_w(x) F'(\eta) \quad (F'(0) = 1) \qquad (25)$$

$$v = u_w(x) (\eta F'(\eta) - 2^{j-1} F(\eta)) \qquad (26)$$

$$g = u_w^2(x) G(\eta) \qquad (27)$$

$$k = u_w^2(x) K(\eta) \qquad (28)$$

$$\epsilon = u_w^3(x) x^{-1} H(\eta) \qquad (29)$$

where the primes denote derivatives with respect to the similarity variable, η, defined by

$$\eta = y/x \qquad (30)$$

and, as defined, $u_w(x)$ is the value of u at the wall. In all that follows the subscript "w" denotes the wall value ($y = 0$, of the associated variable. The function $u_w(x) \ x^{j+1} F(\cdot)$ is the streamfunction of the leading order outer solution. The wall velocity, $u_w(x)$, can be determined from the momentum flux constant, J, by rearranging Eq. (24) into the similarity form

$$u_w(x) = C_J^{1/2} x^{-(j+1)/2} \qquad (31)$$

where C_J is a constant defined by,

$$C_J = \frac{J}{(2\pi)^j} I_2^{-1} \qquad (32a)$$

$$I_2 = \int_0^{\eta_e} F'^2(\eta)\, d\eta \qquad (32b)$$

The similarity equations for momentum, turbulent energy and dissipation are

$$2^{j-1}(F'^2 + F F'') - \left(\frac{K^2 G_\mu}{H} F''\right)' = 0 \qquad (33)$$

$$2^j F'K + 2^{j-1} FK' + \left(\frac{K^2 G_\mu}{\sigma_k H} K'\right)' + \left(\frac{K^2 G_\mu}{H} F''^2\right) - H = 0 \qquad (34)$$

$$\tfrac{1}{2}(5 + 3j) F'H + 2^{j-1} FH' + \left(\frac{K^2 G_\mu}{\sigma_\epsilon H} H'\right)'$$
$$+ c_{\epsilon_1}(KG_\mu F''^2) - c_{\epsilon_2}\left(\frac{H^2}{K}\right) = 0 \qquad (35)$$

The continuity equation is automatically satisfied through the introduction of the "streamfunction", $F(\eta)$. The momentum equation, Eq. (33) can be integrated once, yielding

$$2^{j-1} FF' + \left(\frac{K^2 G_\mu}{H}\right) F'' = 0 \qquad (36)$$

where the wall boundary conditions require the constant of integration to vanish. The eddy viscosity formula for the shear stress takes the form,

$$g/u_w^2 = G = G_\mu(K^2/H) F'' \qquad (37)$$

Results from the numerical solutions of the similarity equations will be presented later in the paper. Although the similarity solution is an exact solution of

the full nonlinear boundary layer equations, it is not an exact similarity as defined in the introduction, because the wall matching conditions require the introduction of additional higher order terms in the outer expansion. Thus the similarity solution described above represents only the leading term of a far field expansion valid for $x \to \infty$, which is an example of what we have called an asymptotic similarity in the introduction.

Limiting Behavior

The asymptotic flow field structure is strongly influenced by the limit behavior of the outer solution for $y \to 0$. A conventional equilibrium wall layer is present near the wall so that the outer solutions, however many layers there may be, must eventually match to a conventional log law for $y \to 0$. The matching will lead to a logarithmic skin friction law of the same type as arises in boundary layers and pipe flows. Since the turbulent shear stress and energy are small in the wall layer then the outer solutions for g and k must vanish at the wall as required by the boundary condition, Eq. (23).

The determination of the correct boundary condition to impose on the dissipation, ϵ, proved considerably more difficult because it was not possible to deduce the proper condition thru a simple scaling analysis. The logarithmic law of the wall requires the dissipation to behave like,

$$\epsilon \sim a^{1/4} \gamma^3 \, y \qquad (38)$$

Thus, the magnitude of ϵ near the wall depends on the length scale of the inner layers and could be: small, order one, or unbounded for $y \to 0$, depending on the thickness and structural form of the inner layers. However, the structure of the flow near the wall, in turn, depends critically on the boundary condition imposed on ϵ and cannot be determined without a knowledge of this condition. Thus the correct wall boundary condition on ϵ and the structure of the solution near the wall can only be determined thru a detailed analysis of the limiting behavior of the outer solution for $y \to 0$ for all possible boundary conditions on ϵ. We first examined the consequences of setting ϵ to zero at the wall. By trial and error we found that the only solution satisfying this condition has the form,

$$u \to u_w(x), \; g \to c_w(x) y, \; k \to A(x) y, \; \epsilon \to B(x) y^{1/2} \quad (39)$$

where $c_w(x)$ is

$$c_w = u_w \frac{du_w}{dx} \qquad (40)$$

and $A(x)$ an $B(x)$ are functions determined from a balance of terms in the turbulent energy and dissipation equations. To lowest order, the dominant terms are provided by a balance of turbulent diffusion, production and dissipation which leads to,

$$A(x) = G_{\mu w}^{-1/2} \left(\frac{\sigma_k - 3\sigma_\epsilon c_{\epsilon_1}}{\sigma_k - 3\sigma_\epsilon c_{\epsilon_2}} \right)^{1/2} |c_w| \qquad (41)$$

$$B^2(x) = \tfrac{1}{2} A^3 G_{\mu w} \left[\frac{1 - (3\sigma_k/\sigma_\epsilon) c_{\epsilon_1}}{\sigma_\epsilon (c_{\epsilon_2} - c_{\epsilon_1})} \right] ; B^2(x) \quad 0 \quad (42)$$

where $G_{\mu w}$ is the limiting value of the turbulent viscosity function at the wall. Since the wall damping function, f, approaches one and the production-dissipation ratio, P/ϵ, approaches a definite limit for $y \to 0$. $G_{\mu w}$ is given by

$$G_{\mu w} = G_\mu[(P/\epsilon)_w, 1] \qquad (43)$$

The functions $A(x)$ and $B(x)$ depend on the model constants. For the standard values given previously, as well as other sensible choices we find that $A(x)$ is strictly positive but that

$$B^2 < 0$$

which demonstrates that solutions of this type, with ϵ equal to zero at the wall, are not possible.

We next considered the possibility that the dissipation was either unbounded or equal to a nonzero constant at the wall. We assumed that the velocity and turbulent shear stress had the same form as in Eq (39) but that the turbulent energy and dissipation had a more general power law variation for $y \to 0$. Thus we assumed the outer solution had the following behavior

$$u \to u_w, \; g \to c_w(x) y, \; k \to A(x) y^a,$$
$$\epsilon \to B(x) y^{-b} \text{ FOR } y \to 0 \qquad (44)$$

where $a > 0$ in order to satisfy the boundary condition on k ($k \to 0$) and $b \geq 0$ in order to avoid the consequences of $\epsilon \to 0$ discussed above. A solution of this type proved possible with the dominant turbulence terms involving a balance of diffusion and dissipation. Turbulent production proved negligible compared to both these terms in this type solution. The balance of the diffusion and dissipation terms resulted in the following expressions for the exponents, a and b.

$$b = 1 - (3/2) a \qquad (45a)$$

$$a = \frac{-7 + (1 + 24\lambda)^{1/2}}{6(\lambda - 2)}, \quad \lambda = (\sigma_\epsilon/\sigma_k) c_{\epsilon_2} \quad (45b)$$

where the positive root in Eq. (45b) was chosen to satisfy the wall boundary condition on k. For the values of model constants used here $a = 0.270$ and $b = 0.595$. Since b is positive the outer solution for the dissipation is unbounded at the wall. A solution with a bounded wall value of ϵ proved to be impossible. The functions $A(x)$, $B(x)$ are to be extracted from the numerical solution of the outer equations for $y \to 0$. The analysis for $y \to 0$ shows that they are related by,

$$A^{3/2} B = a^{-1}(2\sigma_k/3 G_{\mu 0})^{1/2} \qquad (46)$$

The next term in the expansion for u near the wall is determined from an integration of the eddy viscosity equation to yield,

$$u \to u_w(x) + \left\{ \frac{2Bc_w}{(A^2 G_{\mu 0})(2 - a)} \right\} y^{1-a/2} \qquad (47a)$$

where $g_{\mu 0}$ is the limiting value of the viscosity function at the wall defined by,

$$G_{\mu 0} = G_\mu[(P/\epsilon) = 0, 1] \qquad (47b)$$

The boundary conditions Eqs. (22) and (23) completely fix the outer solution, independent of the solution in the inner layers. The general character of the outer solution for the streamwise velocity, u, is as sketched in Fig. 2. The velocity increases monotonically from zero at the upper edge of the jet to a maximum, u_w at the wall. At the upper edge the solution has an algebraic singularity of the same form as in a free jet[19]. At the wall the solution has the singular behavior indicated in Eqs. (44) and (47). Thus the outer solution clearly cannot match the logarithmic behavior of the wall layer, and as a consequence, the skin friction cannot be determined.

8

IV. Diffusion Layer

The analysis of the previous section indicated that the outer solution exhibits an algebraic behavior at the wall, in which the turbulent shear stress and energy vanished while the dissipation becomes unbounded and the velocity approaches a definite limit, $u_w(x)$. Because of the algebraic behavior for $y \to 0$ it is not possible to match the outer solution to the logarithmic law of the wall. This implies that additional layers will be required to achieve a matching to the wall layer solution. The limiting behavior of the outer solution indicates that production and advection of turbulent energy are small for $y \to 0$ resulting in a balance of diffusion and dissipation at the wall. This suggests that we attempt to develop a solution in a thin inner region in which the turbulence characteristics are dominanted by a balance of diffusion and dissipation. Because of the importance of turbulent diffusion in this region we call it the diffusion layer.

The structure of the solution in the diffusion layer is completely determined by the behavior of the turbulent shear stress near the wall. In the outer solution the shear stress is negative with a linear decay to zero at the wall. However the turbulent shear stress is a positive constant in the wall layer equal to the small, $0 (\gamma^2 u(1+j)/2)$ value of the skin friction, τ_w. The outer solution breaks down where the linearly varying shear stress becomes the same order as the wall shear stress. An analysis, not presented here, shows that the breakdown manifests itself through the appearance of a singular contribution in the second-order outer solution for the streamwise velocity. The condition that the linearly varying outer solution for the shear stress is the same order as the wall shear establishes the thickness scale of the diffusion layer to be $\Delta y = 0 (\gamma^2)$. Thus, the solution in the diffusion layer is expressed in terms of the stretched variable, $\tilde{y}$, defined by

$$y = \gamma^2 \tilde{y} \tag{48}$$

Appropriate scalings for all dependent variables follow from the substitution of the stretched variable defined in Eq. (48) into the inner limit of the outer solution given by Eqs. (44) - (47). Thus we are led to solutions of the form

$$U = u_w + \gamma^{2-a} \tilde{u}(x, \tilde{y}) \tag{49}$$

$$g = \gamma^2 (c_w \tilde{y} + \overline{\tau}_w) + \cdots = \tau_{w,r}[c_w \tilde{y} + \overline{\tau}_w] + \cdots \tag{50}$$

$$k = \gamma^{2a}[\tilde{k}(x, \tilde{y})] + \cdots] \tag{51}$$

$$\epsilon = \gamma^{-2b}[\tilde{\epsilon}(x, \tilde{y}) + \cdots] \tag{52}$$

where $c_w(x)$ is the function of u_w defined in Eq. (40) and $\overline{\tau}_w$ is equal to the ratio of wall shear to its reference value,

$$\overline{\tau}_w = \tau_w/\tau_{w,r} \tag{53}$$

Equation (50) follows from an integration of the momentum equation, written in stretched variables. With the scalings given above the turbulent energy and dissipation equations reduce, to lowest order, to a balance of turbulent diffusion and dissipation; a balance that is consistent with the limiting behavior of the outer solution. These equations reduce to second-order ordinary differential equations

for $\tilde{k}$ and $\tilde{\epsilon}$. The only solutions that satisfy these equations and match the outer solution are given by,

$$\tilde{k} = A(x) \tilde{y}^a \tag{54}$$

$$\tilde{\epsilon} = B(x) \tilde{y}^{-b} \tag{55}$$

which are precisely the limiting forms of the outer solution with the functions $A(x)$, $B(x)$ determined from the outer solution and the constants a, b given by Eqs (45). The solution for the streamwise velocity is found by substituting the above expressions for g, k and ϵ into the eddy viscosity formula which yields,

$$\frac{\partial \tilde{u}}{\partial \tilde{y}} = \frac{B}{A^2 G_{\mu_0}} [c_w \tilde{y} - \overline{\tau}_w] \tilde{y}^{-(1+a/2)} \tag{56}$$

where $G_{\mu 0}$ is the zero production limit of the turbulent viscosity function defined in Eq (47b)

The integration of Eq (56) to obtain $\tilde{u}$ introduces an arbitrary function of x into the solution that can be evaluated by matching to the outer solution. The matching requires this function to vanish so that the solution for $\tilde{u}$ can be written in the form,

$$\tilde{u}/\tilde{u}_m = \left[\left(1 - \frac{a}{2} \right) (\tilde{y}/\tilde{y}_m)^{-a/2} + \frac{a}{2} (y/\tilde{y}_m)^{1-a/2} \right] [1 - a]^{-1} \tag{57}$$

where the functions $\tilde{u}_m$ and $\tilde{y}_m$ are,

$$\tilde{u}_m = \left(\frac{4Bc_w}{a(2-a) A^2 G_{\mu_0}} \right) \tilde{y}_m^{(1-a/2)} \tag{58a}$$

$$\tilde{y}_m = \overline{\tau}_w/c_w \tag{58b}$$

since B and $\overline{\tau}_w$ are positive, c_w is negative and $a \approx 0.27$, the function $\tilde{u}_m$ is negative and $\tilde{y}_m$ is postive. It follows that the corresponding two term expansion for the streamwise velocity has a maximum located in the diffusion layer at $\tilde{y} = \gamma^2 \tilde{y}_m$ where the maximum value, U_m, is

$$U_m = u_w + \gamma^{2-a} \tilde{u}_m \tag{59}$$

The second term in Eq. (57) can be shown to match the outer solution given in Eq. (47). The overall behavior of the solution for the velocity profile in the diffusion layer is as sketched in Fig. 2.

Far Field Similarity

The diffusion layer solution can be placed in similarity form by taking note of the similarity forms of the function $A(x)$, $B(x)$, $u_m(x)$, $c_w(x)$ that follow from the definition of c_w in Eq. (40) and similarity solutions given in Eqs (25) - (31). Thus we find

$$A(x) = A_s u_w^2(x) x^{-a} = A_s C_J x^{-(1+J+a)} \tag{60a}$$

$$B(x) = B_s u_w^3(x) x^{b-1} = B_s C_J^{3/2} x^{-(3/2)(1+J+a)} \tag{60b}$$

$$c_w(x) = -(1/2)(1+j) u_w^2(x) x^{-1} = -(1/2)(1+j) C_J x^{-(J+2)} \tag{60c}$$

where A_s, B_s are constants determined from the outer similarity solution and $u_w(x)$ is the similarity

9

form given in Eq. (31). If we define the similarity variable for the diffusion layer by

$$\tilde{\eta} = \bar{y}/\bar{y}_m \qquad (61)$$

the solution for the velocity can be written in the similar form,

$$\tilde{u}/\tilde{u}_m = \left[\left(1 - \frac{a}{2}\right)\tilde{\eta}^{-a/2} - \frac{a}{2}\tilde{\eta}^{1-a/2}\right][1 - a]^{-1} \qquad (62)$$

where, now,

$$\bar{y}_m/x \equiv \Delta_1(x) = 2(j+1)^{-1}(\bar{\tau}_w/u_w^2) \qquad (63a)$$

$$\tilde{u}_m/u_w \equiv \Delta_2(x) = -\left[\frac{2(1+j)^{a/2}B_s}{a(2-a)A_s^2 G_{\mu_0}}\right]\left[\frac{2\bar{\tau}_w}{u_w^2}\right]^{1-a/2} \qquad (63b)$$

and where the term in square brackets is a constant. The x dependence of the functions $\Delta_1(x)$ and $\Delta_2(x)$ appearing in Eqs (63) depends on the solution for the wall shear stress which will be obtained in the next section. The far field solution for the maximum velocity is given in terms of $\Delta_2(x)$ by,

$$U_m = u_w(x)[1 + \gamma^{2-a}\Delta_2(x)] \qquad (64)$$

The solutions for the turbulent energy and dissipation can be arranged into the following similarity form,

$$\tilde{k}/u_w^2 = A_s \Delta_1(x) \tilde{\eta}^a \qquad (65)$$

$$\tilde{\epsilon}\bar{y}_m/u_w^3 = B_s \Delta_1(x)^{1-b}\tilde{\eta}^{-b} \qquad (66)$$

Limiting Behavior

The diffusion layer solution for k and ϵ is given entirely by the terms appearing in the limiting behavior of the outer solution for $y \to 0$, so that the matching of these quantities is obvious. To establish a match between the outer and diffusion layer solutions for the velocity we rewrite the diffusion layer solution, U_D, in outer variables to obtain,

$$U_D = u_{cp} - \gamma^2\left(\frac{2B\bar{\tau}_w}{aA^2 G_{\mu_0}}\right)y^{-a/2} \quad \text{FOR } \bar{y} \to 0 \qquad (67)$$

where the subscripts "D" and "cp" denote the diffusion layer solution and the "common part", the latter being given by the inner limit of the outer solution, Eq (47). The first term in Eq. (67) matches a corresponding term in the outer solution while the second term represents an unbalanced contribution that requires the introduction of an $0(\gamma^2)$ perturbation to the outer solution.

The diffusion layer exhibits an algebraic behavior at the wall that is of the same form as the limiting behavior of the outer solution, except for the velocity which has the general form

$$U_D = u_w(x) - \gamma^2\left(\frac{2B\bar{\tau}_w}{aA^2 G_{\mu_0}}\right)y^{-a/2} \quad \text{FOR } \bar{y} \to 0 \qquad (68a)$$

or, for $x \to \infty$, the similarity form given by

$$U_D = u_w(x)\left\{1 - \gamma^2\frac{\bar{\tau}_w}{u_w^2}\left(\frac{2B_s}{aA_s^2 G_{\mu_0}}\right)\left(\frac{y}{x}\right)^{-a/2}\right\}$$

$$\text{FOR } \bar{y} \to 0 \qquad (68b)$$

Because of the algebraic singularity in Eqs (68) the diffusion layer obviously cannot match the wall layer solution. Thus an additional layer will be required to effect a transition between the algebraic behavior of the diffusion layer solution and the logarithmic behavior of the wall layer solution.

V. Transition Layer and Skin Friction

The thickness of the transition layer is determined from a consideration of the behavior the turbulent energy near the wall. The solution for the turbulent energy in the diffusion layer indicates that it approaches zero like $k \to A\bar{y}^a$ for $\bar{y} \to 0$. Since k is 0 (γ^2) in the wall layer, the diffusion and wall layer solutions for the turbulent energy will be of the same order of magnitude in a layer with a thickness, $\Delta y = 0(\gamma^{2/a})$. Since $a \cong 0.27$, the transition layer is considerably thinner than the diffusion layer and is thicker than the exponentially thin (in terms of γ) wall layer. The solution in the transition layer is expressed in the stretched variable, $\bar{y}$, defined by

$$y = \gamma^{2/a}\bar{y} \qquad (69)$$

The appropriate scalings for the dependent variables in the transition layer follow from the substitution of the stretched variable defined in Eq. (69) into the inner limit of the diffusion layer solution. Thus we seek solutions in the transition layer in the form.

$$g = \gamma^2[\bar{\tau}_w(x) + O(\gamma^{(2/a)-2})] \qquad (70)$$

$$k = \gamma^2[\bar{k}(x, \bar{y}) + \cdots] \qquad (71)$$

$$\epsilon = \gamma^{-2b/a}[\bar{\epsilon}(x, \bar{y}) + \cdots] \qquad (72)$$

$$U = u_w(x) + \gamma\bar{u}(x, \bar{y}) + \cdots \qquad (73)$$

Substitution of these expansions into the turbulent energy, dissipation and eddy viscosity equations yields the following system of ordinary differential equations,

$$\frac{\partial}{\partial\bar{y}}\left(\frac{G_\mu}{\sigma_k}\frac{\bar{k}^2}{\bar{\epsilon}}\frac{\partial\bar{k}}{\partial\bar{y}}\right) = (\bar{k}^2 - \bar{\tau}_w G_\mu^{-1})(\bar{\epsilon}/\bar{k}^2) \qquad (74)$$

$$\frac{\partial}{\partial\bar{y}}\left(\frac{G_\mu}{\sigma_\epsilon}\frac{\bar{k}^2}{\bar{\epsilon}}\frac{\partial\bar{\epsilon}}{\partial\bar{y}}\right) = (C_{\epsilon_2}\bar{k}^2 - C_{\epsilon_1}\bar{\tau}_w G_\mu^{-1})(\bar{\epsilon}^2/\bar{k}^3) \qquad (75)$$

$$\frac{\partial\bar{u}}{\partial\bar{y}} = \frac{\bar{\epsilon}\bar{\tau}_w}{\bar{k}^2 G_\mu} \qquad (76)$$

Equation (70) indicates that the turbulent shear stress is constant across the transition layer to lowest order. Then, by matching to the wall layer solution it is established that the lowest order term for g is equal to the skin friction, $\bar{\tau}_w$, as normalized in Eq. (53). The wall damping function, f, is also equal to one across the transition region, as in the diffusion layer, but here the production-dissipation ratio, P/ϵ, is variable to lowest order. Thus, the viscosity function, G_μ, is determined from the implicit relation,

$$G_\mu = G_\mu\{P/\epsilon, 1\} \qquad (77)$$

$$P/\epsilon = (\bar{\tau}_w^2/\bar{k}^2)G_\mu^{-1} \qquad (78)$$

Equations (74) - (78) are to be solved subject to boundary conditions determined by matching the solution to the diffusion layer for $\bar{y} \to \infty$, and to the law of the wall for $\bar{y} \to 0$. That the transition layer

10

equations admit a log law behavior for $y \to 0$ follows from the fact that all three turbulence source terms: production, dissipation, and diffusion appear in the lowest order description. It is the balance of these terms in the k - ϵ model that leads to the standard log law at the wall. In order to the match to the diffusion layer the solution must also satisfy the following asymptotic conditions.

$$\bar{k} \to A\bar{y}^a \qquad \text{FOR } y \to \infty \qquad (79a)$$

$$\bar{\epsilon} \to B\bar{y}^{-b} \qquad \text{FOR } y \to \infty \qquad (79b)$$

$$\bar{u} \to -\left(\frac{2B\bar{\tau}_w}{aA^2 G_{\mu_0}}\right)\bar{y}^{-a/2} \quad \text{FOR } y \to \infty \qquad (79c)$$

In order to complete the solution and to determine the skin friction the transition layer must match to the logarithmic law of the wall for $\bar{y} \to 0$. In the present notation this leads to the following matching conditions,

$$\bar{u} \to (\sqrt{\bar{\tau}_w}/\kappa_1)(\ln \bar{y}\bar{c}(x)) \text{ FOR } \bar{y} \to 0 \qquad (80a)$$

$$\bar{k} \to \bar{k}_w = \tau_w G_{\mu w}^{-1/2} \qquad (80b)$$

$$\bar{\epsilon} \to \bar{\tau}_w^{3/2}/\kappa, \bar{y} \qquad (80c)$$

where $\bar{\tau}_w$ is the local value of the normalized skin friction, $\bar{c}(x)$ is a function to be extracted from the numerical solution of the transition layer equations and κ_1 is a constant related to the standard von Karmen constant, $\kappa = 0.43$, by the relation

$$\kappa_1 \equiv \alpha^{-1/4}\kappa \qquad (81)$$

which for $\alpha = 0.09$ results in a value $\kappa_1 = 0.79$

The six conditions given in Eqs. (79) and (80) are sufficient to completely solve the fifth order system of ordinary differential equations given by Eqs. (74) - (76) and to determine the solution for the skin friction. However the system of equations is highly nonlinear and must be solved by numerical methods.

Similarity.

Equations (74) - (76) can be considerably simplified by first switching independent variables from $\bar{y}$ to $\bar{u}$ and then placing the resulting equations in similarity form through the following scale transformation.

$$\bar{u} = \sqrt{k_w/\sigma_k}\ \zeta \qquad (82)$$

$$\bar{k} = k_w K(\zeta) \qquad (83)$$

$$\bar{\epsilon} = e E(\zeta) \qquad (84)$$

$$\bar{y} = \frac{\bar{\tau}_w}{e}\sqrt{\frac{k_w}{\sigma_k}}\ Y(\zeta) \qquad (85)$$

where k_w is the value of k at the wall, as given by the law of wall matching condition, Eq. (80b) and e is an arbitrary constant, to be determined by matching to the diffusion layer solution for $\bar{y} \to \infty$. In the following ζ will be taken as the independent variable which is strictly positive and ranges from ∞ at the wall ($\bar{y} = 0$) and to $\zeta = 0$ in the far field ($\bar{y} \to \infty$). The turbulent viscosity function is expressed in the form,

$$G_\mu = G_{\mu w}\bar{G}(P/\epsilon, 1) \qquad (86a)$$

$$P/\epsilon = (K^2\bar{G})^{-1} \qquad (86b)$$

where $G_{\mu w}$ is the value of G_μ at the wall, so that $\bar{G}$ is equal to one for $\bar{y} = 0$. In terms of this transformation the turbulent energy and dissipation equations are,

$$K'' - \bar{G}K^2 = -1 \qquad (87)$$

$$E'' - \beta(K)E = 0 \qquad (88a)$$

where β (K) is defined by

$$\beta(K) = (\sigma_\epsilon/\sigma_k)(c_{\epsilon_2}\bar{G}K - c_{\epsilon_1}K^{-1}) \qquad (88b)$$

The transformation for Y (ζ) is obtained from an integration of Eq. (76),

$$Y = \int_\zeta^\infty (\bar{G}K^2/E)\,d\zeta \qquad (89)$$

where we have imposed the boundary condition,

$$y \to \infty\ (\bar{u} \to -\infty)\ \text{for}\ Y \to 0$$

in order to match the law of the wall.

The transformation removes all parameters from the problem definition, aside from turbulence model constants, so that K (ζ) and E (ζ) are universal functions that need be computed just once for each set of chosen model constants. More importantly, the transformation completely decouples the nonlinear equation for the turbulent energy, K (ζ), from the second order linear equation governing E (ζ). Thus the solution can be obtained sequentially by first solving Eq (87) for K (ζ), next Eq (88) for E (ζ) and finally Eq (89) for Y (ζ). The boundary conditions on K (ζ) are determined by matching to the diffusion layer solution for $\zeta \to 0$ ($y \to \infty$) and to the wall layer solution for $Y \to \infty$ ($y \to 0$). Detailed analysis indicates that the far field matching condition can be satisfied by,

$$K(\zeta) \to \infty \qquad \text{FOR } \zeta \to 0\ (\bar{y} \to \infty) \qquad (90)$$

Because of the chosen scaling on k, the boundary condition at the wall is given by

$$K(\zeta) \to 1 \qquad \text{FOR } \zeta \to \infty\ (\bar{y} \to 0) \qquad (91)$$

The boundary conditions Eqs. (90) and (91) enable Eq. (87) to be integrated once the viscosity function G is specified. Because $\bar{G}(K)$ is a fairly complex function that is defined by an implicit relation (Eq. 86) the turbulent energy equation, Eq. (86), must in general be integrated numerically. A simple exact analytic solution satisfying the boundary conditions can be found for the special case that $\bar{G}(K)$ is a constant equal to its value at the wall. In this case, $\bar{G}(K) = 1$ and K (ζ) is found by integration.

$$K(\zeta) = 3\left[\frac{1 + e^{-\zeta/2}}{1 - e^{-\zeta/2}}\right] - 2 \qquad (92)$$

This turns out to a good approximation even when G is variable, as given by the expression in Ljuboja and Rodi[13] and serves as a good initial estimate for the iterative solution for K (ζ) in the general case.

The solution for K (ζ) determines the function β (K), appearing in the differential equation for

11

$E(\zeta)$. This equation is a second-order linear ordinary differential equation which can be solved as initial value problem using far field boundary conditions determined from the matching conditions to the diffusion layer solution for $\zeta \to 0$ $(\bar{y} \to \infty)$ given by Eq. (79b). Equation (88a) has two power law type solutions for $\zeta \to 0$, one decaying and the other unbounded. In order to match to the diffusion layer the unbounded component must be excluded by imposing the far boundary condition,

$$E(\zeta) \to 0 \qquad \text{FOR } \zeta \to 0 \ (\bar{y} \to \infty) \qquad (93)$$

The solution can be completely determined by prescribing the coefficient of the decaying component. Because of the arbitrary coefficient, e, introduced in the definition of E by Eq (84) we may, without loss in generality, set this coefficient to unity. Thus the second boundary condition on $E(\zeta)$ is taken as,

$$\lim_{\zeta \to 0} (E \zeta^{-a_1}) = 1 \qquad (94)$$

where the exponent, a_1, is determined from the differential equation,

$$a_1 = 2b/a \sim 4.40 \qquad (95)$$

where a, b are the parameters appearing in the outer solution as defined by Eq. (45). These conditions enable us to compute $E(\zeta)$ as a simple initial value problem by marching the solution from $\zeta = 0$ to $\zeta \to \infty$. However, we found it more convenient to solve the E equation as a two point boundary value problem using the same computer code used to compute $K(\zeta)$. The velocity profile $\bar{u}(\bar{y})$ is determined implicitly via Eq. (82) and the transformation function, $Y(\zeta)$, is evaluated by a numerical integration of Eq. (89). The scale function, e, for the dissipation is evaluated by matching the transition layer solution for ϵ to the far field limit given in Eq. (79b). This completes the determination of the solution in the transition layer in terms of the local value of the skin friction. The skin friction is then evaluated by carrying out the matching of transition and wall layer solutions.

Limiting Behavior and Evaluation of the Skin Friction

The parameter, e, scaling the dissipation is determined by matching the transition solution to the diffusion layer. For $\zeta \to 0$, $(\bar{y} \to \infty)$ the solution behaves as,

$$\bar{k} \to (6k_w/\bar{G}_\infty)\zeta^{-2} \qquad \text{FOR } \zeta \to 0 \ (\bar{y} \to \infty) \qquad (96)$$

$$\bar{\epsilon} \to e\zeta^{2b/a} \qquad \text{FOR } \zeta \to 0 \ (\bar{y} \to \infty) \qquad (97)$$

$$\bar{y} \to (\bar{\tau}_w e^{-1} d^{-3a/2b})\zeta^{-2/a} \qquad \text{FOR } \zeta \to 0 \ (\bar{y} \to \infty) \qquad (98)$$

where $\bar{G}_\infty$ is the limiting value of $\bar{G}$ in the far field and is given by

$$\bar{G}_\infty = G_{\mu 0}/G_{\mu w} \qquad (99a)$$

where

$$G_{\mu w} = G_\mu (P_w/\epsilon_w, 1) \qquad (99b)$$

and d is the constant,

$$G_{\mu 0} = G_\mu (0, 1) \qquad (99c)$$

$$d = \left[\frac{18a \, G_{\mu w}^{3/4}}{\sigma_k^{1/2} G_{\mu 0}}\right]^{-2b/3a} \qquad (100)$$

Equations (96) - (98) can be inverted to give explicit expressions for the far field behavior of the transition solution in terms of the physical coordinate, $\bar{y}$. The resulting expressions match the limiting forms of the diffusion layer solution, given in Eqs. (79), if the arbitrary function, e, scaling the dissipation is given the value,

$$e = d\bar{\tau}_w^{-b/a} B^{2/3a}(x) \qquad (101)$$

where $B(x)$ is the known function that arises in the inner limit of the outer solution (Eq. 42).

The matching to the diffusion layer solution and the boundary condition $k \to k_w$ completely determines the solution in the transition layer in terms of the unknown value of the skin friction, τ_w. This is determined, and the solution completed by matching the transition layer solution to the logarithmic law of the wall.

In the present notation the law of the wall solution in the inner layer is expressed in the form,

$$U^*/u_j^* = u_\tau F^+(y_+), \quad y^+ = yu_\tau Re_j \qquad (102)$$

For $y^+ \to \infty$ this reduces to the standard log law,

$$U^*/u_j^* \to u_\tau(x) [\kappa^{-1} \ln (yu_\tau(x) Re_j) + C_b^+] \quad \text{FOR } y_+ \to \infty \quad (103)$$

where C^+ is the standard constant $(C^+ \sim 5)$ in the logarithmic law of the wall. For $\zeta \to \infty$ $(y \to 0)$ the limiting solution for the turbulent energy approaches its value at the wall, exponentially in ζ,

$$\bar{k}_0 \to \bar{k}_w [1 + O(e^{-\sqrt{2}\zeta})] \qquad \text{FOR } \zeta \to \infty \quad (104)$$

while the dissipation ϵ and coordinate transformation, $\bar{y}(\zeta)$, approach the limits

$$\bar{\epsilon}_0 \to e E_s e^{-\beta_w \zeta} \qquad \text{FOR } \zeta \to \infty \quad (105)$$

$$\bar{y} \to \frac{\bar{\tau}_w}{e E_s} \sqrt{\frac{\bar{k}_w}{\sigma_k \beta_w}} \, e^{-\beta_w \zeta} \qquad \text{FOR } \zeta \to \infty \quad (106)$$

where β_w is a constant equal to the limiting value of $\beta(K)$ at the wall and is given by the following expression involving only the turbulence model constants,

$$\beta_w = (\sigma_\epsilon/\sigma_k)(c_{\epsilon 2} - c_{\epsilon 1}) \qquad (107)$$

The parameter E_s is a constant to be determined from the numerical solution for $E(\zeta)$ for $\zeta \to \infty$. Inverting these expressions we obtain,

$$\bar{\epsilon} \to \bar{\tau}_w^{3/2} \kappa_1 \bar{y}^{-1} \qquad (108)$$

$$\bar{u} \to \frac{\sqrt{\bar{\tau}_w}}{\kappa_1} [\ln (\bar{y} e E_s \kappa_1 / \bar{\tau}_w^{3/2}) + O(1)] \qquad (109)$$

where κ_1 must satisfy the relation

$$\kappa_1^2 = G_{\mu,w}^{1/2} \sigma_\epsilon (c_{\epsilon 2} - c_{\epsilon 1}) \qquad (110)$$

This is just one of the standard relations, written in the present notation, used to fix the model constants in the $k - \epsilon$ model to assure that it satisfy the standard log law at the wall (eg see Ref. 20). Equations (104), (108) - (110) demonstrates that the transition layer solution matches to the wall layer solution. Using Eq. (109) the transition solution for the ve-

locity profile near the wall can be written in the form,

$$U = u_w(x) + \frac{\sqrt{\tau_w}}{\kappa \alpha^{3/4}} \ln[y\, dE_s\, B^{2/3a} \kappa_1 \alpha^{(1+j)/2a} \tau_w^{-1/a}] \qquad (111)$$

comparing this expression to the outer limit of the wall layer solution given by Eq. (103) yields the following implicit relation for the skin friction

$$\Lambda^{-1} - (1 + 2a^{-1}) \ln \Lambda = (1 + 2a^{-1}) \ln u_w(x) - \ln \theta(x)$$
$$+ [\ln \alpha^{(1+j)/4} Re_j + \kappa C^*] \qquad (112)$$

where the skin friction τ_w is given in terms of Λ and u_w by

$$\tau_w / u_w^2(x) = \alpha^{j/2} \kappa^2 \Lambda^2(x) \qquad (113)$$

and $\theta(x)$ is the function defined by,

$$\theta(x) = d\, E_s \kappa_1^{-2/a} B^{2/3a}(x) \qquad (114)$$

In the far field limit, $x \longrightarrow \infty$, $\theta(x)$ approaches the following limit

$$\theta(x) = \theta_s C_J^{1/a} x^{-(1+j+a)/a} \qquad (115a)$$

where

$$\theta_s = d\kappa_1^{-2/a} E_s B_p^{2/3a} \qquad (115b)$$

and B_s is the constant appearing in the similarity expression for $B(x)$ given in Eq. (60a). Using this relation and the similarity form for $u_w(x)$ given in Eq. (31) we can write the far field asymptotic solution for $\Lambda(x)$ in the form,

$$\Lambda^{-1} - (1 + 2a^{-1}) \ln \Lambda =$$
$$[\ln(\alpha^{(1+j)/4} Re_j C_J^{1/2} \theta_s^{-1} x^{(1-j)/2}) + \kappa C^*] \qquad (116)$$

where C_J is the normalized momentum flux defined in Eq. (32). Equation (116) expresses the solution for the skin friction in the far field similarity region in terms of the momentum flux constant, C_J, the jet Reynolds number, Re_j, turbulence model constants and two constants B_s and E_s which are determined by numerical solution for the outer (free jet) region and transition layer equations. It is interesting to note that the local skin friction coefficient, $c_F \equiv \tau_w/$ $(1/2) u_w^2$, is exactly constant for a radial wall jet ($j = 1$) and varies logarithmically in x for the planar jet ($j = 0$). The above formula for the skin friction admits an interesting similarity that will be discussed in the next section.

Results

The similarity form for the radial and planar outer layer and the transition layer have been solved numerically for $G_\mu = 1$ as well as for the algebraic stress model of Ljuboja and Rodi[13], here denoted by $G_\mu \neq 1$. Product composites of the form

$$U = U_{OUTER} \frac{[U_{DIFF} + U_{TRANS} - CP_{DIFF/TRANS}]}{CP_{OUTER/DIFF}} \qquad (117)$$

where CP denotes the common part of the subscripted layers, are used to compare the present asymptotic solutions with respect to the numerical solutions of Ljuboja and Rodi.[13] These results are also compared with "universal" correlations of experimental data proposed by Narasimba et al. for plane wall jets.

The equations governing the outer layer are

solved by the method of Paullay et al.[19] Application of an independent variable transformation, $\zeta = \zeta(\eta)$ such that

$$\frac{d\eta}{d\xi} = G_\mu \frac{K^2}{H} \qquad (118)$$

acts to decouple the kinetic energy and dissipation equations as well as to reduce much of the non-linearity of the system. In the new coordinate the bounds $\xi \rightarrow -\infty, +\infty$ replace $\eta = 0$, η_e and, the location of the finite edge is found a posteriori by quadrature, viz.

$$\eta_e = \int_{-\infty}^{\infty} G_\mu \frac{K^2}{H} d\xi \qquad (119)$$

The numerical solution is obtained by central differencing the transformed equations and using the edge and wall asymptotic behavior as two-point boundary values. Repeated application of tridiagonal solvers to the system of equations allows for their convergence to levels of local residuals no greater than 10^{-11}.

Results for the outer solution in the planar case with $G_\mu = 1$ (Fig. 3) are compared with the corresponding free jet solutions.[19] For reasons discussed previously, the radial and planar wall jet solutions have the identical similarity form as the free jet flow. It is apparent that the effect of the wall is to reduce the velocity half-width by about 30%. The behavior of the mean and turbulent variables are essentially the same in the edge region of the layer but differ significantly near $\eta \rightarrow 0$ where wall jet dissipation becomes unbounded and the turbulent energy and eddy viscosity go to zero. The results for radial jets are qualitatively the same as for the planar case.

The mean velocity deficit, $\bar{u}/\bar{u}m$, profile in the diffusion layer (Fig. 4) is given analytically by Eq (57) and it exhibits the local maximum that characterizes wall jets.

Solutions to the transition layer must, in general, be obtained numerically and again central differences are employed to represent Eqs (87,88) subject to boundary conditions Eq (90,91) and initial conditions Eq (93,94), respectively. In practice K^{-1} is used as the dependent variable in Eq (87) and the difference equations are solved from $\zeta = 0$ ($\bar{y} \rightarrow \infty$) to some finite cutoff, $\zeta = \zeta_c$, chosen large enough for a two term large ζ expansion to prevail. Since the dissipation equation, Eq (88), is homogeneous, it may be solved as a two-point boundary value problem with E set to zero at $\zeta = 0$, Eq (93) and to an arbitrarily prescribed value at the edge $\zeta = \zeta_c$. The resulting numerical solution is then rescaled to comply with Eq (94). This procedure enabled us to solve for K and E simultaneously on the same mesh to the same level of precision. The numerical results are indistinguishable from the analytical solution for $K(\zeta)$, Eq (92), that is available for $G_\mu = 1$. The more general algebraic stress model[13] (i.e. $G_\mu \neq 1$) gives results (Fig. 5) that are very close to those obtained with the standard (i.e. $G_\mu = 1$) turbulence model. It should be recalled that the $Y(\zeta)$ curve is actually a stretched velocity profile (Eqs 82,89).

The numerical solutions for the outer layer and the transition layer provide the constants (Table 1) required for asymptotic matching with the diffusion layer. It has been established that all numerical solutions exhibit the correct asymptotic behaviors for $\eta \rightarrow \eta_e$, 0 and $\zeta \rightarrow 0, \infty$ with the exponents predicted to within 1% of their analytical values.

a) VELOCITY

b) TURBULENT SHEAR STRESS
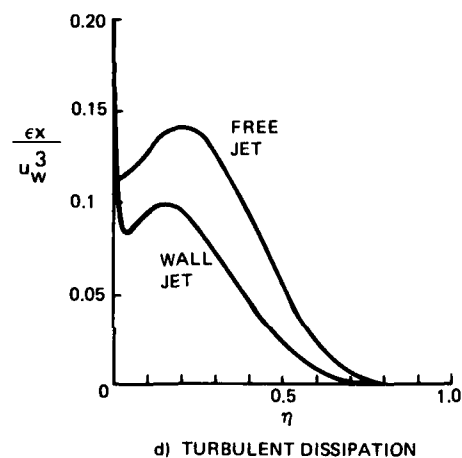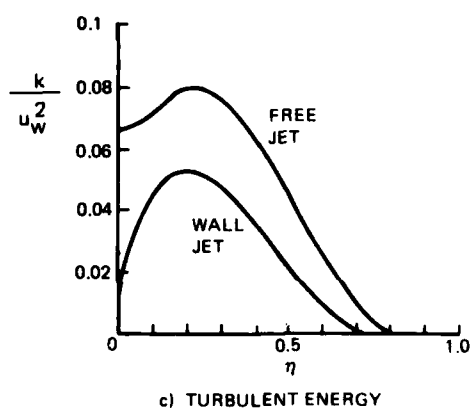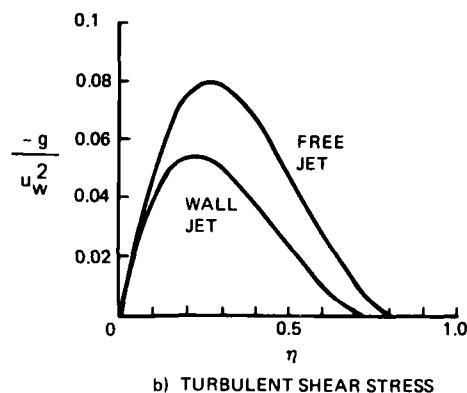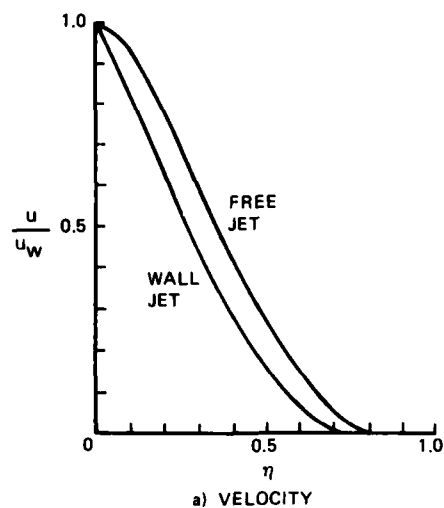
c) TURBULENT ENERGY

d) TURBULENT DISSIPATION

Fig. 3 Plane Jet/Wall Jet Outer Layer Similarity Profiles ($G_\mu = 1$)

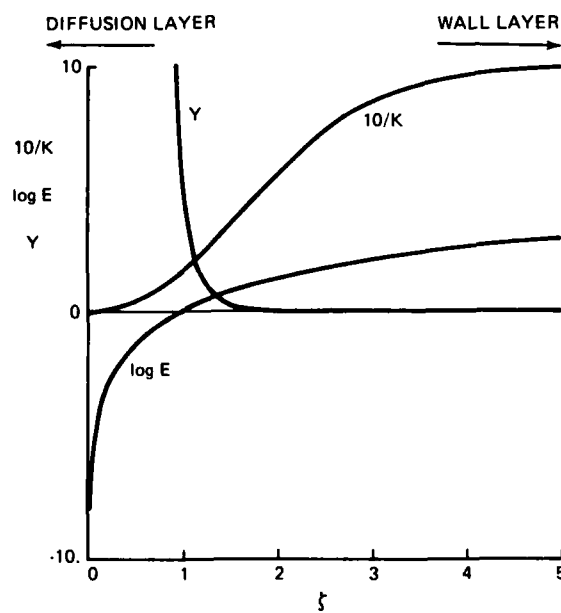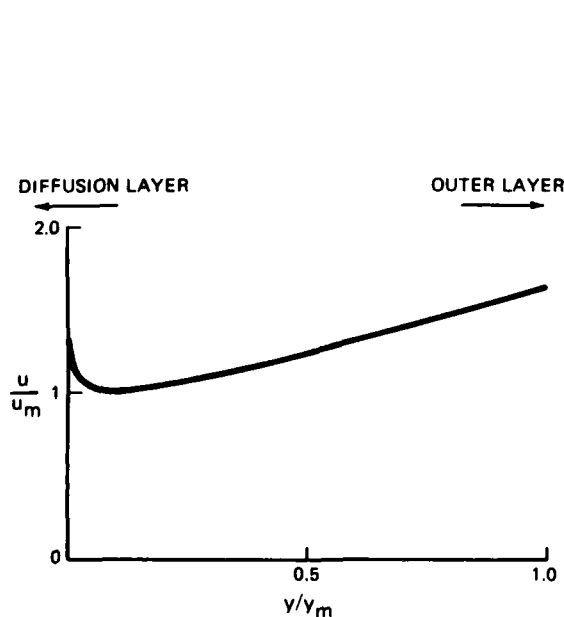Fig. 4 Diffusion Layer Velocity Profile ($G_\mu = 1$)

Fig. 5 Transition Layer Solution ($G_\mu = 1$)

14

TABLE 1 Computed Constants in the Similarity Solutions

TURBULENCE MODEL	GEOMETRY	A_s	B_s	E_s	I_2
STANDARD WITH $C_\mu = 0.09$	PLANAR	.0635	5.30×10^{-3}	18.96	.1899
	RADIAL	.1106	1.218×10^{-2}	18.96	.1308
MODIFIED WITH $C_\mu = C_\mu (P/\epsilon, f)$	PLANAR	.0337	1.370×10^{-3}	12.45	.0932
	RADIAL	.0575	3.05×10^{-3}	12.45	.0591

In order to use these results to generate the solution profiles for specific wall set flows the skin friction must first be evaluated from Eq (116). It is convenient to rewrite this equation in the form

$$\Lambda^{-1} - (1 + 2a^{-1}) \ln \Lambda = \tfrac{1}{2} \ln \mathcal{J} + \{\tfrac{1}{2} \ln(\alpha I_2 \theta_s^{-2}) + \kappa C^*\} \quad (120)$$

where
$$\mathcal{J} = \frac{J^* r^{*1-j}}{(2\pi)^j \rho^* \nu^{*2}} = \frac{J}{(2\pi)^j} (\alpha^{-1/2} x)^{1-j} Re_j^2 \quad (121)$$

This formulation demonstrates that for the radial wall jet the skin friction coefficient, Λ, is a constant that depends only on the jet Reynolds number and turbulence model constants; for a plane wall jet Λ is variable that depends on the logarithm of the streamwise coordinate, x. The solution to Eq (120) is presented (Fig. 6) for radial and plane wall jets and for $G_\mu = 1$, $G_\mu \neq 1$. As expected, Λ decays slowly with J. For the data to be examined here J is in the $10^9 < J < 10^{12}$ range where $\Lambda \simeq 0.1$.

A solution corresponding to Ljuboja and Rodi's[13] numerical result at $r^*/b^* = 200$ (x = 60) ($Re_j = 1.8 \times 10^4$, J = 6.48 x 10^{10}) is developed using their algebraic Reynolds stress model ($G_\mu \neq 1$). The composite solution for velocity is presented in Fig. 7, along with the outer and transition layer calculations in order to indicate the overall nature of the matching. The large gap between the outer and composite solutions apparent in this result is an indication of the importance of higher order terms in the outer

Fig. 7 Structure of Composite Solution — Plane Wall Jet ($G_\mu \neq 1$, $\Lambda = 0.100$)

solution. The velocity profile merges with the law of the wall behavior at about y + = 20 (Fig. 8) which is close to the patching location used by Ljuboja and Rodi. Since the law of the wall region extends out to about y + $\approx$ 20 these results indicate that typical solutions exhibit a logarithmic law of the wall behavior only over a very limited interval. This marginal log law region is consistent with the experimental observations[8,10,12] discussed previously. The mean velocity, turbulent shear stress and energy profiles obtained[13] by a parabolic marching integration of the partial differential equations are in reasonable agreement with composite for field solution calculated here (Fig. 9).

Fig. 6 Friction Velocity as a Function of Wall Jet Momentum Parameter from Transition Layer Matching with Law of the Wall.
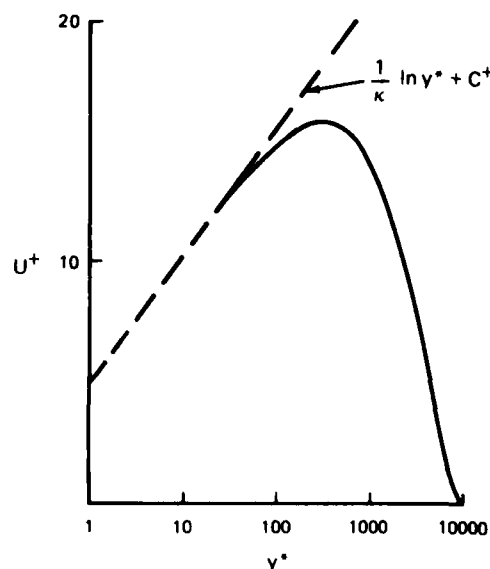
Fig. 8 Composite Solution Match with Law of the Wall — Plane Wall Jet ($G_\mu = 1$, $\Lambda = 0.100$, $\kappa = 0.43$, $C^+ = 5.0$)
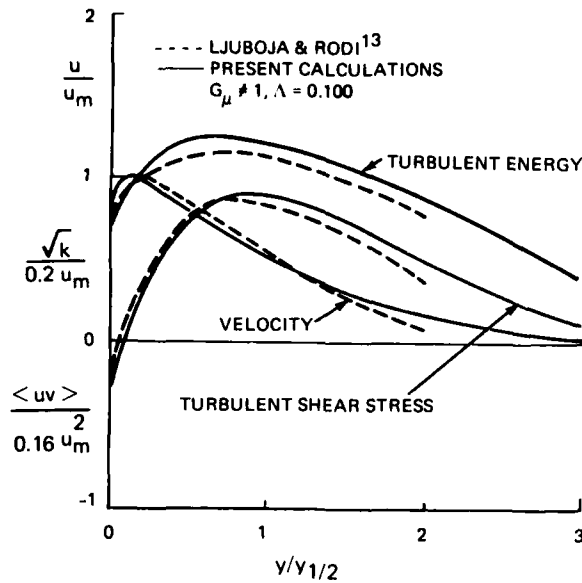
Fig. 9 Comparison of Asymptotic Composite Solution with Parabolic Matching Result for Plane Wall Jet

order terms in the outer layer. The model constants used in the algebraic stress model of Ref. 13 are not consistent with the law of wall compatability condition given by Eq (110). In order to have the outer layer turbulence model conform to that of Ljuboja and Rodi, Eq (110) is used throughout to locally determine $c_{\varepsilon 2}$ as a function of G_μ. Numerical experiments carried out here and by Rodi[21] indicate negligible effects due to this slight inconsistency in their model.

A dimensional analysis performed by Narasimha et al.[18] suggests that plane wall jets are described by their initial momentum and the kinematic viscosity. Together these quantities provide unique length and velocity scales $[L^*] = [\gamma^{*2}/J^*]$, $[U^*] = [J^*/\gamma^*]$. For the radial wall jet this is not the case since J^*/γ^{*2} is itself dimensionless. The results obtained here conform to the analysis of Narasimha et al. The plane wall jet shear stress is determined only by the value of $\mathcal{J}$ (Eq 120, Fig 6). The streamwise behavior of the scaled mean and turbulence quantities are universal functions of $\mathcal{J}$ which serves as a scaled streamwise coordinate in the planar case. (Fig. 10a-d). Comparison of the present planar results with the proposed universal curves[18] show good agreement for velocity maximum decay (Fig. 10a). The present results for the maximum velocity were computed from the composite solution given in Eq (117) rather than from the analytic expression given

Agreement is good in the region near the wall and deteriorates toward the edge of the wall jet, which is another indication of the need for including higher
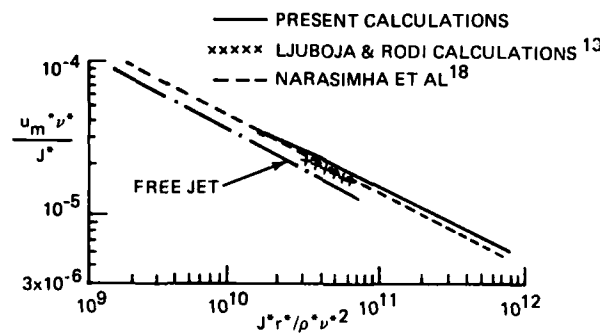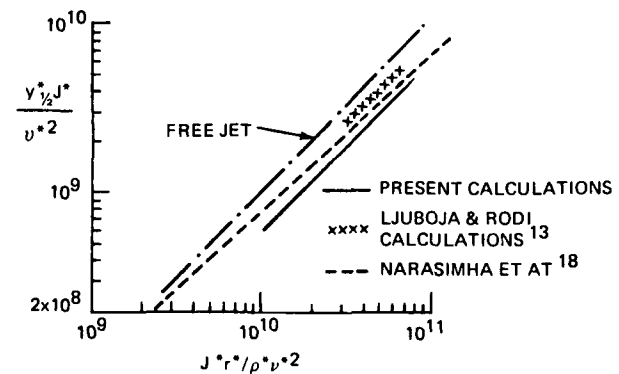
a) MAXIMUM VELOCITY

b) VELOCITY HALF-WIDTH
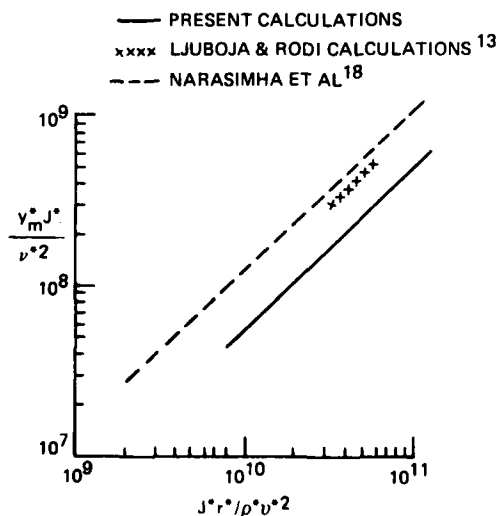
c) MAXIMUM VELOCITY LOCATION

$$\frac{\tau_w^* \nu^{*2}}{J^{*2}} = \frac{\Lambda^2 \kappa_1^2}{I_2} \frac{\rho^* \nu^{*2}}{J^* r^*}$$
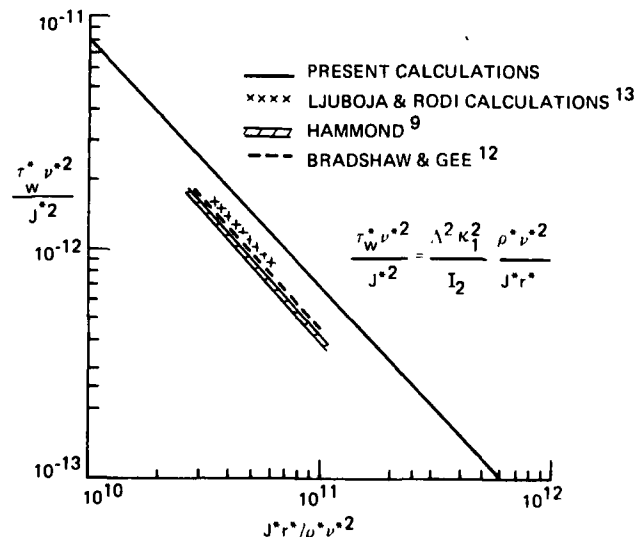
d) WALL SHEAR STRESS

Fig. 10 Streamwise Variation of Scaling Parameters — Plane Wall Jets

by the diffusion layer solution, Eq (64). The velocity half-widths are underpredicted by 30% (Fig. 10b). The calculation of Ljuboja and Rodi agree with Narasimha giving further cause to surmise that higher order term terms in the outer layer are important. The velocity half-width is expected to be quite sensitive to such terms. The height above the wall, y_m^*, of the velocity maximum is considerably underpredicted by the composite solution (Fig. 10c) and this is partly explained by the use of an eddy viscosity model which forces this point to be collocated with the zero shear stress point. Since the vanishing shear stress location is observed to fall between the wall and the velocity maximum, some underprediction is expected. Still, the computations of Ljuboja and Rodi are considerably closer to the universal curve of Narasimha et al. The behavior of the wall shear stress (Fig. 10d) is of particular note. Narasimha et al give no such result but Hammond[9] correlates wall shear stress with a scaling based upon slot height. Here the Hammond result for skin friction is rescaled and compared with our analytic solution, Eq (120), the calculations of Ljuboja and Rodi[13] and the observations of Bradshaw and Gee[22]. The agreement of the latter with the proposed curve of Hammond is a direct result of our rescaling. The Bradshaw and Gee[12] result did not correlate well with the original scaling due to Hammond[9]. The present solution shows the correct variation of the wall shear with distance but overpredicts its level by about 40% again suggesting a sensitivity of Eq (120) to higher order terms in the outer layer. Nevertheless, the results presented here confirm (at least to lowest order) that the scaling of Narasimha et al.[18] does indeed provide a universal correlation for the far field of a plane wall jet. Interestingly, radial wall jets have already been shown to possess far field composite profiles (i.e. across the entire wall jet) that depend only upon their initial momentum (i.e. idependent of streamwise distance). Although plane jet far field profiles vary slowly with streamwise distance, their streamwise decay is described by a universal function of a single variable dependent on initial momentum and distance while those of radial wall jets are not. The lack of such universality for radial wall jets as well as the spareseness of far field observations precludes their comparison with the composite solution at the present time.

VI. Conclusions and Discussion

The present paper describes a new analytical approach for analyzing turbulent plane and radial wall jets. The method is based on a systematic two parameter asymptotic expansion using a k-ε turbulence model. One of the parameters, γ, is related to the friction velocity and controls the Reynolds number effects induced by the solid wall; the other parameter, α, is equal to the model constant appearing in the eddy viscosity formula and controls the turbulent shear stress levels in the outer free jet part of the wall jet. The α expansion leads to the usual boundary layer approximation while the γ expansion leads to a four layer structure of the wall jet for $\gamma \to 0$. The theory is valid in a region downstream from initial zone where the wall jet is formed. We have determined the equations and matching conditions governing the leading term of the expansion in each layer. The theory leads to explicit expressions for the magnitude and position of the maximum velocity in the wall jet and for the shear stress at the wall. Similarity solutions have been developed for each layer to describe the limiting behavior of the wall jet far downstream. Complete solutions of the leading order similarity equations

in each layer have been obtained for plane radial jets with both the standard k-ε turbulence model (constant c_μ) and for the Ljuboja and Rodi [13] algebraic reynolds stress model. The present solutions for the plane wall jet where compared with Ljuboja and Rodi's numerical solution of the boundary layer and k-ε model equations and with Narasimha, Yenga Narayan and Parthasarathy's[18] experimental correlations.

The main conclusions of the present work are:

- The wall jet develops a four layer structure for $Re_j \to \infty$. The multi-layer structure is a consequence of the turbulent shear stress in the outer layer being large compared to the shear stress levels in the inner wall layer. We believe this structure is a general feature of other turbulent shear flows that have relatively high turbulent shear stress levels in the outer region.

- The outer region of a wall jet is similar to a free jet. The present theory shows that the overall momentum flux in a wall jet is constant to lowest order, as it is in a free jet and that the similarity form of the outer region of the wall jet is similar to a free jet with the same velocity and length scales to lowest order. The present theory provides a theoretical explanation of why the observed variation of the velocity and length scales of wall jets are so close to those of free jets. Nevertheless, the presence of the solid surface is felt in the outer flow through the boundary conditions on the turbulent energy and dissipation. Thus the outer solution in the present theory is not a free jet as in Glauert's theory. The behavior or the outer solution near a wall is dominated by the vanishing of the turbulent viscosity at the wall and consequently the profiles in the outer solution differ significantly from the symmetrical profiles of a free jet.

- The structural form of the wall jet solution is sensitive to the turbulence model. It is the use of the dissipation equation that leads to the requirement for a four layer structure. The length scale in the "extra" transition region is sensitive to the model constants in the k-ε model through their influence on the parameter α. The four layer structure for this type of flow (i.e. large turbulent shear stress levels in outer part of shear layer) may be a general property of the dissipation equation. Although not demonstrated here, it can be shown that for a prescribed algebraic length scale the extra transition region is not required and a three layer structure evolves. The consequences of this observation for turbulence modeling remains to be established.

- The present theory indicates dominance of turbulent diffusion near the wall. The diffusion layer is a productionless zone that is dominated by a balance of diffusion and dissipation to lowest order. Again, this may be a general feature of flows with relatively large turbulent shear stress levels in the outer region.

- The velocity maximum occurs in the diffusion layer. Solution profiles in the diffusion layer are described by simple analytic expressions that follow from the linear shear stress variation across the layer and from the balance of diffusion and dissipation. Simple expressions are found for the magnitude and position of the maximum velocity in the wall jet. The expression for the maximum velocity is exactly similar for a radial wall jet but is not for a plane wall jet where there is an additional weak logarithmic dependence on the streamwise distance.

- The wall jet has an asymptotic similarity form that describes the flow far downstream. The leading order terms are exactly similar for $x \to \infty$. Deviations from exact similarity arise from higher order terms in the asymptotic expansions. The present theory accounts only for leading order similar terms.

- The present theory is consistent with a conventional law of the wall in the innermost layer. Because of the rapid changes across the diffusion and transition layers the extent of the overlap region, in which the velocity profile is well represented by a conventional logarithmic law of the wall, is small, which is generally consistent with experimental observations. The present theory shows that this diminished overlap region is due to the large gradients of shear stress normal to the wall. The present theory indicates that this reduces the extent of the log law region but does not eliminate it.

- The theory leads to a solution for the skin friction in the form of a standard log law. A general explicit expression for the skin friction is deduced for the intermediate streamwise zone (i.e. $x = 0(1)$) of the wall jet where the outer solution is described by partial differential equations. The solution involves one unknown function $B(x)$ that must be determined from the numerical solution of the outer layer partial differential equations. A completely determined solution for the skin friction is deduced for the asymptotic far field similarity region ($x \to \infty$). The local skin friction coefficient, defined in terms of local values of $U_w(x)$ or $U_m(x)$, is shown to be constant for radial jets and to depend on log x for plane jets.

- The present theory provides the basis for the scaling analysis that Narasimha, Yenga Narayan, and Parthasarathy [18] used to successfully correlate plane wall jet data. The present theory leads to the same similarity variables deduced by these authors on the basis of dimensional analysis and shows that the plane wall jet solution depends only on a suitably defined non-dimensional momentum flux. The theory explains why a similar type dimensional analysis does not work for radial wall jets.

- Comparisons of the present solutions for plane wall jet profiles shows relatively good agreement with Ljuboja and Rodi's numerical solutions of the boundary layer equations. The solution for the decay of the maximum velocity also shows good agreement with Ljuboja and Rodi's computations and with the experimental correlations of Ref. 18.

The present paper was limited to the development of the overall asymptotic approach and to the computation of the leading order terms. Initial comparisons of the present theory with "exact" numerical calculations [13] and with experimental correlations [18] for plane wall jets shows that it correctly predicts many features of these flows. However, these comparisons also indicate, (Figs. 10b, c), that the present first order theory significantly underpredicts the spread rates $\delta_{1/2}$ and δ_m of both the half velocity and maximum velocity and maximum velocity points, respectively. Although the overall variation with downstream distance is correctly predicted, due mainly to similarity considerations, the absolute magnitudes are not. The same is true, to a lesser degree, for the skin friction predictions (Fig 10d). These discrepancies are indicative of the importance of the neglected second-order terms in the expansions. The relatively large gap between the outer and composite solutions for the velocity apparent in the results of Fig. 7 is indicative of the magnitude of neglected second-order effects.

The present theory is based on the $k-\varepsilon$ turbulence model, which employs an eddy viscosity model for the turbulent shear stress. Although the $k-\varepsilon$ model cannot adequately describe the details of the flow near the points of maximum velocity and zero shear stress, Ljuboja and Rodi show that their $k-\varepsilon$ formulation can predict most other features of wall jet flows on flat surfaces, where these two points are close together. As indicated by Gibson and Younis[14], the points of maximum velocity and zero shear stress become more widely separated on curved surfaces; these flows cannot be well predicted with an eddy viscosity formulation. However, Gibson and Younis show that a significantly improved description of the flow near a velocity maximum can be achieved with a Reynolds stress model (RSM) of turbulence that incorporates a wall damping term of the type used by Ljuboja and Rodi. The asymptotic approach described in the present paper can be directly applied to the Gibson and Younis RSM equations. Since the RSM employs the same dissipation equation used in the present study the theory will lead to the same four layer structure as in present work. The use of a RSM can be expected to give a significantly improved description of the solution in the diffusion layer. It would be useful to determine whether the four layer structure is a general feature of flows with an outer region of large Reynolds shear stress or if it is simply a consequence of the particular form chosen for the dissipation equation.

We have carried out only limited comparisons of the theory with experimental data. It is certainly desirable to continue these studies and to perform more extensive comparisons. Howver, before proceeding with futher applications, it would appear best to compute the second-order terms to determine if they improve the predictions of spread rate and skin friction levels.

VIII. References

1. Townsend A.A., The Structure of Turbulent Shear Flow, 2nd ed., Cambridge University Press, New York, 1976, pp. 268-271.

2. Ibid, pp. 195-230, pp. 262-276.

3. Rotta, J.C., "Turbulent Boundary Layers in Incompressible Flow," Progress in Aero. Sci, 2 ed., A. Ferri, D. Kuchemann and L.H.G. Sterne, Pergamon Press, Oxford, 1962, pp 1-219.

4. Rodi, W., The Prediction of Free Turbulent Boundary Layers by Use of a Two-Equation Model of Turbulence, Ph.D. Thesis, University of London, 1972.

5. Schlichting, H., Boundary Layer Theory, 7th ed., McGraw Hill Book Co., New York 1979, Chapter XXIV.

6. Glauert, M.B. "The Wall-Jet" J. Fluid Mech., 1, 1956, pp. 625-643.

7. Bakke, P., "An Experimental Investigation of a Wall Jet," J. Fluid Mech., 2, 1957, pp.467-472.

8. Poreh, M., Tsuei, Y.G. and Cermak, J.E., "Investigation of a Turbulent Radial Wall Jet," Trans. ASME, J. Appl. Mech., 89, 1967, pp. 457-463.

9. Hammond, G.P., "Complete Velocity Profile and "Optimum" Skin Friction Formulas for the Plane Wall-Jet," Trans. ASME, J. Fluids Eng., 104, 1982, pp. 59-66.

10. Schwarz, W.H. and Cosart, W.P., "The Two Dimensional Turbulent Wall Jet," J. Fluid Mech, 10, 1961, pp. 481-495.

11. Meyers, G.E., Schauer, J.J. and Eustis, R.W., "The Plane Turbulent Wall Jet, part I," Trans. ASME, J. Basic Eng., 85, 1963, pp. 47-54.

12. Bradshaw, P. and Gee, M.T., "Turbulent Wall Jets with and without an External Stream," ARCR&M 3252, 1960.

13. Ljuboja, M. and Rodi, W., "Calculation of Turbulent Wall Jets with an Algebraic Reynolds Stress Model," Trans. ASME, J. Fluid Eng., 102, 1980, pp. 350-356.

14. Gibson, M.M. and Younis, B.A., "Modeling the Curved Turbulent Wall Jet," AIAA J., 20, 1982, pp. 1707-1712.

15. Launder, B.E. and Rodi, W., "Turbulent Wall Jet," 1980-81 AFOSR-HTTM-Stanford Conference on Complex Turbulent Flows, ed. S.J. Kline, B.J. Cantwell and G.M. Lilley, Stanford University, 1981, pp. 434-456.

16. Adamson, T.C. and Messiter, A.F., "Analysis of Two-Dimensional Interactions Between Shock Waves and Boundary Layer," Ann Rev. Fluid Mech, 12, 1980, pp. 103-138.

17. Melnik, R.E., "Turbulent Interactions on Airfoils at Transonic Speeds - Recent Developments," AGARD Conference of Computation of Viscous - Inviscid Interactions, CP-291, Paper No. 10, Colorado Springs, Co, Sept. 1980.

18. Narasimha, R., Yenga Narayan, K. and Parthasarathy, S.P., "Parametric Analysis of Turbulent Wall Jets in Still Air.,"Aeronautical J., 77, 1973, pp. 355-359.

19. Paullay, A.J., Melnik, R.E., Rubel, A., Rudman, S and Siclari, M.J., "Similarity Solutions for Plane and Radial Jets Using a K-E Turbulence Model" (submitted to JFM).

20. Rodi, W., Turbulence Models and Their Application in Hydraulics, IAHR-Section on Fundamentals of Divison II; Experimental and Mathematical Fluid Dynamics, 1980, p 28.

21. Rodi, W., Private Communication Nov., 1982.

Technical Library
Building 313
Ballistic Research Laboratories
Aberdeen Proving Ground, MD 21005

Mr. Aviars Celmins
Ballistic Research Laboratory
Ballistic Modelling Division
Aberdeen Proving Ground, MD 21005

Dr. P.J. Roache
Ecodynamics Research Associates,
Inc.
P.O. Box 8172
Albuquerque, NM 87108

Defense Technical Information Center
CAmeron Station, Building 5
Alexandria, VA 22314   12 copies

Library
Naval Academy
Annapolis, MD 21402

Director, Tactical Technology Office
Defense Advanced Research Projects
  Agency
1400 Wilson Boulevard
Arlington, VA 22209

Code 200B
Office of Naval Research
800 N. Quincy Street
Arlington, VA 22217

Code 438
Office of Naval Research
800 N. Quincy Street
Arlington, VA 22217   2 copies

Dr. J.L. Potter
Deputy Director, Technology
von Karman Gas Dynamics Facility
Arnold Air Force Station, TN 37389

Professor J.C. Wu
School of Aerospace Engineering
Georgia Institute of Technology
Atlanta, GA 30332

Library
Aerojet-General Corporation
6352 North Irwindale Avenue
Azusa, CA 91702

NASA Scientific and Technical
Information Facility
P.O. Box 8757
Baltimore/Washington International
Airport, MD 21240

Dr. K.C. Wang
College of Engineering
San Diego State University
San Diego, CA 92182

Professor A.J. Chorin
Department Mathematics
University of California
Berkeley, CA 94720

Professor M. Holt
Department of Mechanical Engineering
University of California
Berkeley, CA 94720

Dr. H. R. Chaplin
Code 1600
David W. Taylor Naval Ship Research
  and Development Center
Bethesda, MD 20084

Dr. Hans Lugt
Code 1802
David W. Taylor Naval Ship Research
  and Development Center
Bethesda, MD 20084

Dr. Francois Frenkeil
Code 1802
David W. Taylor Naval Ship Research
 and Development Center
Bethesda, MD   20084

Dr. T.C. Tai
Code 1506
David W. Taylor Naval Ship Research
 and Development Center
Bethesda, MD   20084

Professor C.H. Lewis
Department of Aerospace and Ocean
 Engineering
Virginia Polytechnic Institute and
 State University
Blacksburg, VA   24061

Professor A.H. Nayfeh
Department of Engineering Science
Virginia Polytechnic Institute and
 State University
Blacksburg, VA   24061

Commanding Officer
Office of Naval Research
Eastern/Central Regional Office
665 Summer Street, Bldg. 114,
Section D
Boston, MA   02210

Dr. J.C. Erickson, Jr.
CALSPAN Corporation
Advanced Technology Center
P.O. Box 400
Buffalo, New York   14225

Dr. T.J. Falk
CALSPAN Corporation
Advanced Technology Center
P.O. Box 400
Buffalo, New York   14225

Dr. C. Witliff
CALSPAN Corporation
Advanced Technology Cnter
P.O. Box 400
Buffalo, New York   14225

Professor R. F. Probstein
Department of Mechanical Engineering
Massachusetts Institute of
Technology
Cambridge, MA   02139

Commanding Officer
Officer of Naval Research Branch
Office
536 South Clark Street
Chicago, IL   60605

Code 753
Naval Weapons Center
China Lake, CA   93555

Mr. J. Marshall
Code 4063
Naval Weapons Center
China Lake, CA   93555

Professor R.T. Davis
Department of Aerospace Engineering
University of Cincinnati
Cincinnati, OH   45221

Professor S.G. Rubin
Department of Aerospace Engineering
 and Applied Mechanics
University of Cincinnati
Cincinnati, OH   45221

Library MS 60-3
NASA Lewis Research Center
21000 Brookpark Road
Cleveland, OH   44135

Dr. J.D. Anderson, Jr.
Chairman, Department of Aerospace
 Engineering
College of Engineering
University of Maryland
College Park, MD   10742

Professor O. Burggraf
Department of Aeronautical and
 Astronautical Engineering
Ohio State University
1314 Kinnear Road
Columbus, OH   43212

Technical Library
Naval Surface Wapons Center
Dahlgren Laboratory
Dahlgren, VA 22448

Dr. F. Moore
Naval Surface Weapons Center
Dahlgren Laboratory
Dahlgren, VA 22448

Technical Library 2-51131
LTV Aerospace Corporation
P.O. Box 5907
Dallas, TX 75222

Library, United Aircraft Corporation
 Research Laboratories
Silver Lane
East Hartford, CT 06108

Dr. W.R. Briley
Scientific Research Associates, Inc.
P.O. Box 498
Glastonbury, CT 06033

Professor P. Gordon
Calumet Campus
Department of Mathematics
Purdue University
Hammond, IN 46323

Library (MS 185)
NASA Langley Research Center
Langley Station
Hampton, VA 23665

Professor A. Shapmann
Chariman, Mechanical Engineering
 Department
William M. Rice Institute
Box 1892
Houston, TX 77701

Technical Library
Naval Ordnance Station
Indian Head, MD 20640

Professor D.A. Caughey
Sibley School of Mechanical and
 Aerospace Engineering
Cornell University
Ithaca, NY 14850

Professor E.L. Resler
Sibley School of Mechanical and
 Aerospace Engineering
Cornell Univeristy
Ithaca, NY 14850

Professor S.F. Shen
Sibley School of Mechanical and
 Aerospace Engineering
Cornell University
Ithaca, NY 14850

Library
Midwest Research Institute
425 Volker Boulevard
Kansas City, MO 64110

Dr. J.J. Riley
Flow Research, Inc.
P.O. Box 5040
Kent, WA 98031

Dr. S.A. Orszag
Cambridge Hydrodynamics, Inc.
54 Baskin Road
Lexington, MA 02173

Dr. P. Bradshaw
Imperial College of Science and
 Technology
Department of Aeronautics
Prince Consort Road
London SW7 2BY, England

Professor T. Cebeci
Mechanical Engineering Department
California State University, Long
 Beach
Long Beach, CA 90840

Dr. H.K. Cheng
University of Southern California
Department of Aerospace Engineering
University Park
Los Angeles, CA 90007

Professor J.D. Cole
Mechanics and Structures Department
School of Engineering and Applied
 Science
University of California
Los Angeles, CA 90024

Dr. Charles Watkins
Head, Mechanical Engineering Dept.
Howard University
Washington, DC   20059

Dr. A.L. Slafkosky
Scientific Advisor
Commandant of the Marine Corps
 (COde AX)
Washington, D.C.   20380

Director
Weapons Systems Evaluation Group
Washington, DC   20350

Research Library
AVCO Corporation
Missile Systems Division
201 Lowell Street
Wilmington, MA   01387

AFAPL (APRC)
AB
Wright Patterson Air Force Base,
OHIO   45433

Dr. Donald J. Harney
AFFDL/FX
Wright Patterson Air Force Base,
OHIO   45433

Flow Research
1320 Fenwick Lane
Suite 401
Silver Spring, MD   20910

Scientific Officer
Program Director Fluid Dynamics
Mathematical and Information
Sciences
Office of Naval Research
800 North Quincy Street
Arlington, VA   22217

Attn: Dr. Robert E. Whitehead
        Code 438
Ref: N00014-81-C-0549

Director, Naval Research Laboratory
Attn: Code 2627
Washington, DC   20375   6 copies

Administrative Contracting Officer
Bethpage, L.I., New York 11714

END

FILMED